Targeting the Delivery of Glycan-Based Paclitaxel Prodrugs to Cancer Cells via Glucose Transporters

Yih-Shyan Lin,[†,‡] Rudeewan Tungpradit,[†,§] Supachok Sinchaikul,[†] Feng-Ming An,[†] Der-Zen Liu,[||] Suree Phutrakul,[§] and Shui-Tein Chen*[,†,‡]

Institute of Biological Chemistry and Genomics Research Center, Academia Sinica, Taipei, 11529, Taiwan, Institute of Biochemical Sciences, National Taiwan University, Taipei, 10617, Taiwan, Department of Chemistry, Faculty of Science, Chiang Mai University, Chiang Mai, 50200, Thailand, and Graduate Institute of Biomedical Materials, Taipei Medical University, Taipei, 110, Taiwan

Received May 26, 2008

This report describes the synthesis of four novel paclitaxel based prodrugs with glycan conjugation (**1**−**4**). Glycans were conjugated using an ester or ether bond as the linker between 2′-paclitaxel and the 2′-glucose or glucuronic acid moiety. These prodrugs showed good water solubility and selective cytotoxicity against cancer cell lines, but showed reduced toxicity toward normal cell lines and cancer cell lines with low expression levels of GLUTs. The ester conjugated prodrug **1** showed the most cytotoxicity among the prodrugs examined and could be transported into cells via GLUTs. Fluorescent and confocal microscopy demonstrated that targeted cells exhibited morphological changes in tubulin and chromosomal alterations that were similar to those observed with paclitaxel treatment. Therefore, these glycan-based prodrugs may be good drug candidates for cancer therapy, and the glycan conjugation approach is an alternative method to enhance the targeted delivery of other drugs to cancer cells that overexpress GLUTs.

Introduction

Recently, target-specific drug delivery has become a promising strategy to improve the selectivity of cytotoxic drugs toward targeted cells. In this system, a carrier for a specific cellular target is conjugated with the drug to form a prodrug which is less toxic than that of the parent drug. The carrier has two roles. One is to reduce the toxicity of the drug to normal cells, and the other is to enhance the specificity of the drug for candidate cells. After the prodrug gets to the target cell, the drug is released from its inactive form (or less toxic form) to an active form that performs its physiological functions. This concept has been successfully applied to the development of many chemotherapy agents. One such example is antibody directed enzyme prodrug therapy (ADEPT[a]), in which an antibody bound enzyme is targeted to tumor cells. For cancer therapy, this allows the nontoxic prodrug to be selectively activated at the tumor site, and the site-selective prodrug activation results in reduced side effects in remote tissues.[1−3] Another approach is gene-directed enzyme prodrug therapy (GDEPT), which is a gene-based, two-step treatment for cancer.[4] In this case, an exogenous gene coding for an enzyme is delivered to cancer cells specifically, and the expressed enzyme can convert a nontoxic prodrug into a cytotoxic species that can kill the cell. Likewise, prodrug monotherapy (PMT) is based on elevated tumor enzymes. For example, β-glucuronidase plays a role in the degradation of glycosaminoglycans that contain glucuronic acid, and it can activate low-toxic prodrugs to become highly cytotoxic agents specifically at the tumor site.[5−8] These enzymes are overexpressed in many malignancies, yet present at relatively low concentrations in normal tissues, thus, curbing activation of the prodrug in nontargeted tissues. Indeed, this enzymatic pathway has been a promising candidate in PMT.[4,9−11]

Glucose uptake into tissues or cells is mainly performed by GLUTs, a family of membrane proteins. Cancer cells generally express higher levels of GLUTs than normal cells.[12−16] This is because the efficiency of ATP production in normal cells does not satisfy the high energy requirements of cancer cells, so GLUTs are overexpressed in cancer cells to improve glucose uptake. This differential rate of glucose uptake has been used in positron emission tomography (PET), whereby 2-[18F]-2-deoxy-D-glucose (FDG) (a glucose analogue) accumulates in cancer cells and indicates the tumor position.[17,18] The ratio of GLUT expression in malignant verses normal cells is about 100−300, which makes the noise peaks and background signal of the tumor analysis very reliable. FDG uptake and GLUTs expression is well-correlated in multiple malignant cells, such as colon, breast, and lung carcinomas.

Paclitaxel, a diterpenoid taxane derivative, is one of most potent anticancer agents used in clinical practice today.[19,20] It possesses a unique mechanism of action by binding tubulin and stabilizing microtubule formation, which ultimately disrupts mitosis and causes cell death.[21−23] However, some drawbacks of paclitaxel hamper its clinical usefulness. For example, paclitaxel lacks selective cytotoxicity toward cancer cells. Thus, both normal and cancerous cells may be affected, and this may lead to unwanted side effects.[24] The poor water solubility of paclitaxel is another problem that seriously reduces its wider clinical application. Although many attempts have been made

* To whom correspondence should be addressed. Dr. Shui-Tein Chen, Institute of Biological Chemistry, Academia Sinica, 128 Academia Rd., Sec. II, Nankang, Taipei, 11529, Taiwan. Tel: +886-2-27886230. Fax: +886-2-27883473. E-mail: bcchen@gate.sinica.edu.tw.

† Institute of Biological Chemistry and Genomics Research Center, Academia Sinica.

‡ National Taiwan University.

§ Chiang Mai University.

|| Taipei Medical University.

[a] Abbreviations: ADEPT, antibody directed enzyme prodrug therapy; DCC, dicyclohexylcarbodiimide; DMAP, 4-dimethylaminopyridine; DMF, dimethyl formamide; DMSO, dimethyl sulfoxide; EtOAc, ethyl acetate; FBS, fetal bovine serum; FCS, fetal calf serum; GDEPT, gene-directed enzyme prodrug therapy; FDG, 2-[18F]-2-deoxy-D-glucose; GLUTs, glucose transporters; MeOH, methanol; MEME, minimum essential medium eagle; MTT, 3-(4,5-dimethylthiazol-2-yl)-2,5-diphenyltetrazolium bromide; NaH, sodium hydride; PBS, phosphate buffer saline; PDC, pyridium dichromate; PET, positron emission tomography; PMT, prodrug monotherapy; Pyr, pyridine; RP-HPLC, reverse phase-high performance liquid chromatography; TBAF, tetrabutylammonium fluoride; TBAI, tetrabutylammonium iodide; TESCl, triethylchlorosilane; THF, tetrahydrofuran

10.1021/jm8006257 CCC: $40.75
Published on Web 11/16/2008

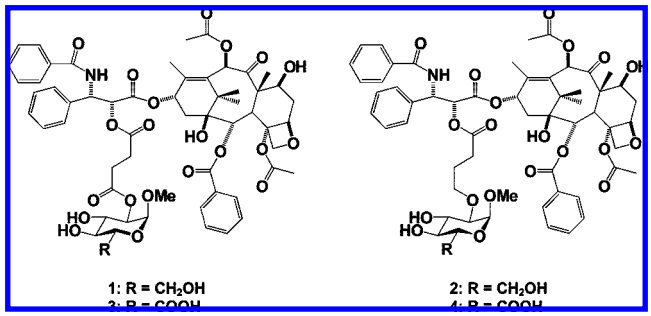

Figure 1. Structures of glucose-based (**1** and **2**) and glucuronic acid-based (**3** and **4**) paclitaxel prodrugs.

to improve the solubility of paclitaxel, such as using detergents or Cremophor EL, these have caused hypersensitivity or related side effects in patients.[25]

In this study, we developed two glucose and two glucuronic acid-derived paclitaxel prodrugs: **1**, **2**, **3**, and **4** (for structures, see Figure 1). These prodrugs were designed to take advantage of the increased GLUT expression and β-glucuronidase activity of cancer cells. We expected that these prodrugs would be similar to FDG, which is specifically delivered into cells via GLUT uptake. We used seven cancer cell lines (NCI-H838, Hep-3B, A498, MES-SA, HCT-116, NPC-TW01, and MKN-45) and two normal cell lines (HUV-E-C and CHO-K1) to determine the toxicity and specificity of these prodrugs compared to paclitaxel. To examine the targeted delivery of the prodrugs, their internalization into cells was analyzed by observing the morphological changes of tubulin and the chromosomal alterations in cancer cells before and after the drug treatment using fluorescent and confocal microscopy.

Chemistry

Two glycans, glucose and glucuronic acid, were conjugated at the 2′-position of paclitaxel through an ester or ether linker at the C2′-hydroxyl group of the glycans. The following four glycan-based paclitaxel prodrugs were obtained: **1**, **2**, **3**, and **4** (Figure 1). In vivo, the covalent bonds of the glycans can be cleaved by intracellular or extracellular enzymes and subsequently expose the carboxylic or hydroxyl group at the terminal position of the spacer. The lone-pair electrons in these functional groups will then react with the carboxylic group at the other side of linker and release paclitaxel.

Procedures for the syntheses of prodrugs **1**−**4** are shown in Schemes 1−4, respectively. A protected glucose, **C14**, was used as the starting material. For synthesis of **1**, the 2′-OH position of **C-14** was treated with succinic anhydride to give **5** with a yield of 71%. **5** was directly conjugated with paclitaxel using DCC/DMAP in pyridine to give **6** with a yield of 71%. In the synthesis of **2**, **C-14** was coupled with a benzoic acid 4-bromobutyl ester. This reaction was catalyzed by NaH/TBAI in DMF to form the ether, **7**, with a yield of 72%. The free hydroxyl group of **8** was obtained by treatment of **7** with 4 N NaOH/MeOH at room temperature for 1.5 h to give **8** in quantitative yield. **8** was oxidized to the carboxylic acid **9** by PDC in DMF with a 50% yield, and **9** was then conjugated with paclitaxel by DCC/DMAP coupling to give **10** with an 80% yield. Hydrogenolysis of **6** and **10** using Pd/C in MeOH generated **1** and **2** with yields of 93% and 95%, respectively. For synthesis of **3**, the 2-hydroxy group of **C-14** was treated with benzoic chloride in pyridine to yield **11** (100% yield). This was followed by the selective release of the 6-hydroxy of **11** catalyzed by aluminum chloride (75% yield). Jones oxidation of the 6-hydroxy group, saponification of the 2-hydroxy, and esterification at the 6-carboxylic acid of **12** gave the glucuronic acid-derivative **13** with a yield of 23% for the three steps. **13** was converted to **14** by treatment with succinic anhydride in pyridine with a yield of 96%. **14** was coupled with paclitaxel in DCC/DMAP/THF (75% yield), which was followed by hydrogenolysis of the protecting groups to give **3**, with a yield of 95%. For synthesis of **4**, **7** was treated with $AlCl_3$ and NEt_3BF_3 in toluene to give **16** (62% yield). Saponification of **16** in NaOH/MeOH followed by Jones oxidation gave **17** (60% yields in both steps). **17** was coupled with paclitaxel by DCC/DMAP in THF to give **18** with a yield of 73%. Hydrogenolyis of **18** generated **4** with a yield of 90%. The prodrugs **1**−**4** were purified by RP-HPLC and the molecular weight was determined by mass spectrometry (*m*/*z*) (Figures S1−S4, Supporting Information). The structures of prodrugs were confirmed by ^{1}H NMR and ^{13}C NMR.

Physical tests found that glucose and glucuronic acid conjugation significantly increased the solubility of paclitaxel in aqueous solution. The solubility of prodrugs **1**, **2**, **3**, and **4** in PBS buffer were 53, 80, 104, and 137 μg/mL, respectively, while the solubility of paclitaxel is less than 0.4 μg/mL. Thus, the solubility of glycan-based prodrugs increased between 130- and 340-fold compared with paclitaxel. The fluorescently labeled paclitaxel derivative was prepared by first protecting the 2-hydroxy group of paclitaxel with TES (84% yield). This was followed by the conjugation of an *m*-aminobenzoic acid to the 7′-position of **19** to give **20** with a yield of 46%. TBAF/THF released the TES protecting group from **20** to generate **21** with a quantitative yield. **23** was obtained by coupling **21** and **5** with DCC/DMAP (85% yield), followed by hydrogenolysis to give **23** (97% yield) (Scheme 5).

Biological Assay Results

Cytotoxicity of Prodrugs against Cancer and Normal Cell Lines. The prodrugs were designed to improve their selective targeting to cancer cells which overexpressed GLUTs, but not to normal cells, which express fewer GLUTs. We chose two normal cells (HUV-EC-C and CHO-K1) and seven cancer cell lines (NCI-H838, Hep-3B, A498, MES-SA, HCT-116, NPC-TW01, and MKN-45) to test the toxicity of prodrugs and compare the results to paclitaxel (Table 1). From the Human Protein Atlas (HPA) database, the GLUTs were highly expressed on NCI-H838, MES-SA, HCT-116, and NPC-TW01 cancer cell lines, but not on Hep-3B, A498, or MKN-45, nor on the normal cells, HUV-EC-C and CHO-K1. In addition, the gene expression levels of GLUT1 and GLUT4 were determined in all cell lines by RT-PCR and the results showed that the expression level of GLUT1, the major GLUT in cancer cells, was higher than its expression level in normal cells (Table 1 and Figure S5, Supporting Information). However, it is also dependent upon the selective cytotoxicity of prodrug against each type of cancer cells.

Among these cell lines, the cytotoxicity of the prodrugs was less than that of paclitaxel. The IC_{50} (concentration for half inhibition of cell growth) of the prodrugs was modulated by the amount of GLUTs expressed on both the cancer and normal cells. As shown in Table 1, the growth of NCI-H838, MES-SA, HCT-116, and NPC-TW01 cells was greatly inhibited. However, normal cells and the Hep-3B, A498, and MKN-45 cells were unaffected. The nine cell lines also have different cytotoxic responses to paclitaxel, as shown by their IC_{50}. Interestingly, none of the prodrugs (except prodrug **4**) had any effect on the HUV-EC-C and CHO-K1 cells, whereas paclitaxel inhibited their proliferation. The selectivity index (SI) was

Scheme 1. Synthesis of Glycan-Based Paclitaxel Prodrug **1** Using an Ester Bond as the Linker between Paclitaxel and Glucose[a]

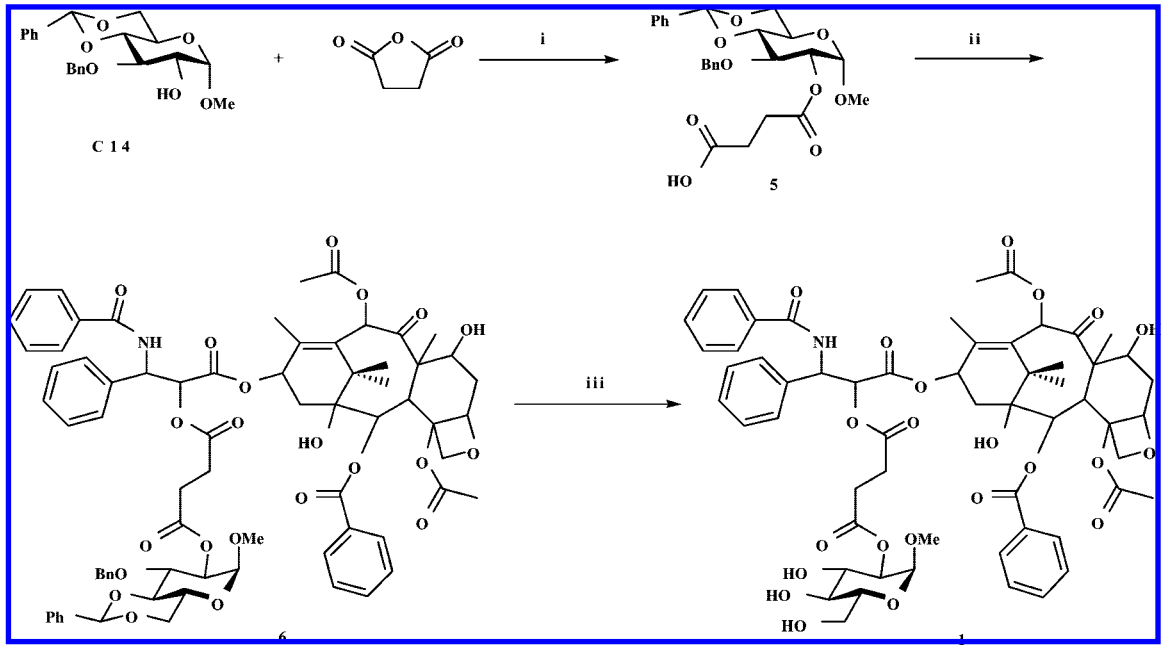

[a] Reagents and conditions: (i) DMAP, Pyr, rt, 12 h, 71%; (ii) Paclitaxel, DCC, DMAP, Pyr, rt, 20 h, 71%; (iii) H_2, Pd/C, MeOH, rt, 12 h, 93%.

Scheme 2. Synthesis of Glycan-Based Paclitaxel Prodrug **2** Using an Ether Bond as the Linker between Paclitaxel and Glucose[a]

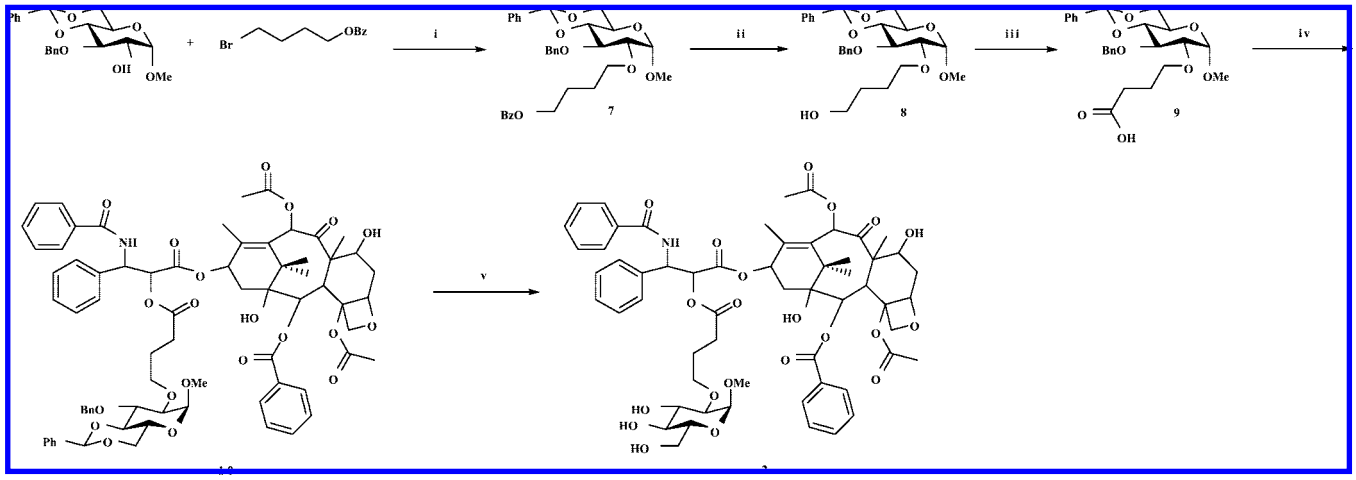

[a] Reagents and conditions: (i) NaH, TBAI, DMF, rt, 36 h, 72%; (ii) NaOH, MeOH, rt, 1.5 h, 100%; (iii) PDC, DMF, rt, 18 h, 50%; (iv) Paclitaxel, DCC, DMAP, THF, rt, 20 h, 80%; (v) H_2, Pd/C, MeOH, rt, 12 h, 95%.

determined by the proportion of the IC_{50} of cancer cells relative to that of normal cells. The SI values of prodrugs **1**, **2**, **3**, and **4** against the NPC-TW01 cell line and two normal cell lines were relatively low (HUV-EC-C cells, $<0.25 \times 10^3$, $<0.78 \times 10^3$, $<0.67 \times 10^3$, and 1.52×10^3, respectively; CHO-K1 cells, $<0.25 \times 10^3$, $<0.78 \times 10^3$, $<0.67 \times 10^3$, and 2.79×10^3, respectively) as compared to that of paclitaxel (HUV-EC-C cells, 1.16×10^3; CHO-K1 cells, 0.38×10^3).

The low toxicity of prodrugs **1**−**3** in normal cells indicated that the conjugations (glucose-ester or ether linkage and glucuronic acid-ester linkage) could reduce the toxicity of paclitaxel and demonstrated the safety of these prodrugs in normal human cells. Among these prodrugs, prodrug **1**, which used a glucose-ester linkage, had the highest cytotoxicity specific to cancer cells and may represent a potent candidate prodrug for further investigation.

Internalization of a Fluorescently Labeled Prodrug into Cancer Cells. To investigate the delivery of prodrugs into cancer cells, compound **23** was conjugated with *m*-aminobenzoic acid (a chromophore group) at the 7′-position on paclitaxel (Scheme 5). This conjugation at the 7′-position of paclitaxel, instead of glucose, was to avoid any physiological changes in the uptake via GLUTs. In addition, this type of modification reportedly does not affect the biological activity of paclitaxel. After the treatment of NPC-TW01 cells with the fluorescently labeled prodrug **1** for 5 h, prodrug **1** could be detected in the cytoplasmic region of NPC-TW01 cells by fluorescence microscopy (Figure 2). According to the colocalization of prodrug **1** and tubulin in NPC-TW01 cells under fluorescence microscopy (Figure 3), this suggested that cancer cells can uptake this glucose-based prodrug into cells. In addition, the rate of internalization of prodrug **1** was very fast (within 5 h), while there were no fluorescent signal in

Scheme 3. Synthesis of Glycan-Based Paclitaxel Prodrug **3** Using an Ester Bond as the Linker between Paclitaxel and Glucuronic Acid[a]

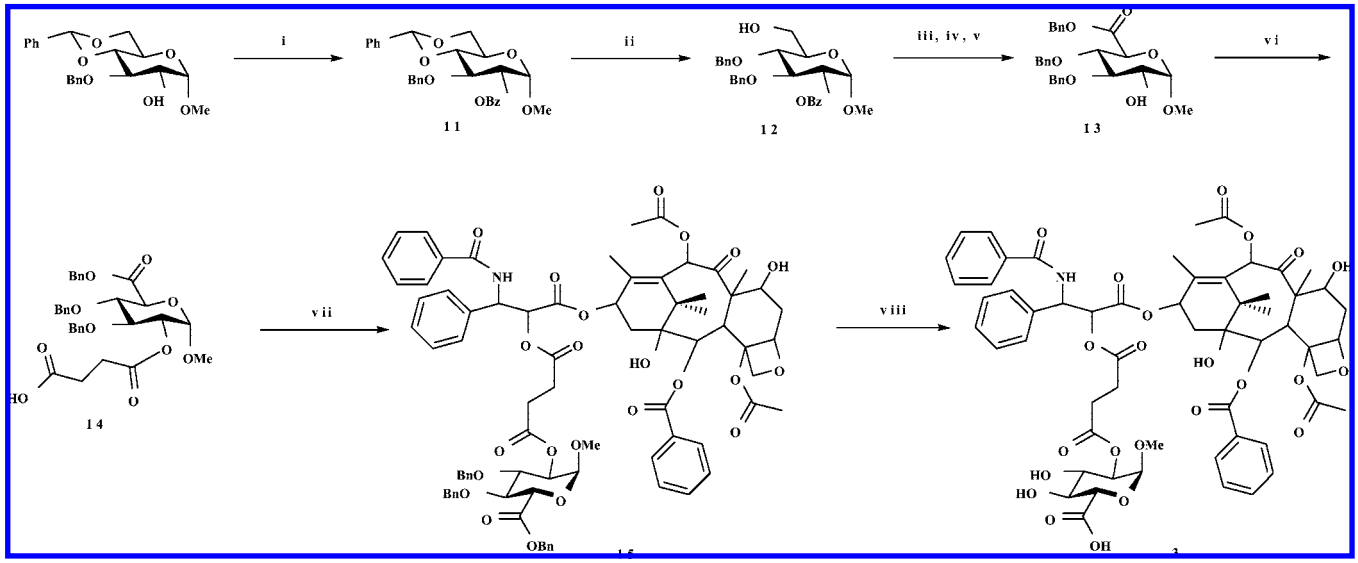

[a] Reagents and conditions: (i) BzCl, Pyr, rt, 12 h, 100%; (ii) $AlCl_3$, NEt_3BF_3, toluene, 0 °C, 20 min, 75%; (iii) Jones reagent, rt, 18 h; (iv) NaOH, MeOH, rt, 4 h; (v) BnOH, DCC, DMAP, THF, rt, 18 h, 3 steps, 23%; (vi) succinic anhydride, Pyr, rt, 12 h, 96%; (vii) paclitaxel, DCC, DMAP, THF, rt, 18 h, 75%; (viii) H_2, Pd/C, MeOH, rt, 12 h, 95%.

Scheme 4. Synthesis of Glycan-Based Paclitaxel Prodrug **4** Using an Ether Bond as the Linker between Paclitaxel and Glucuronic Acid[a]

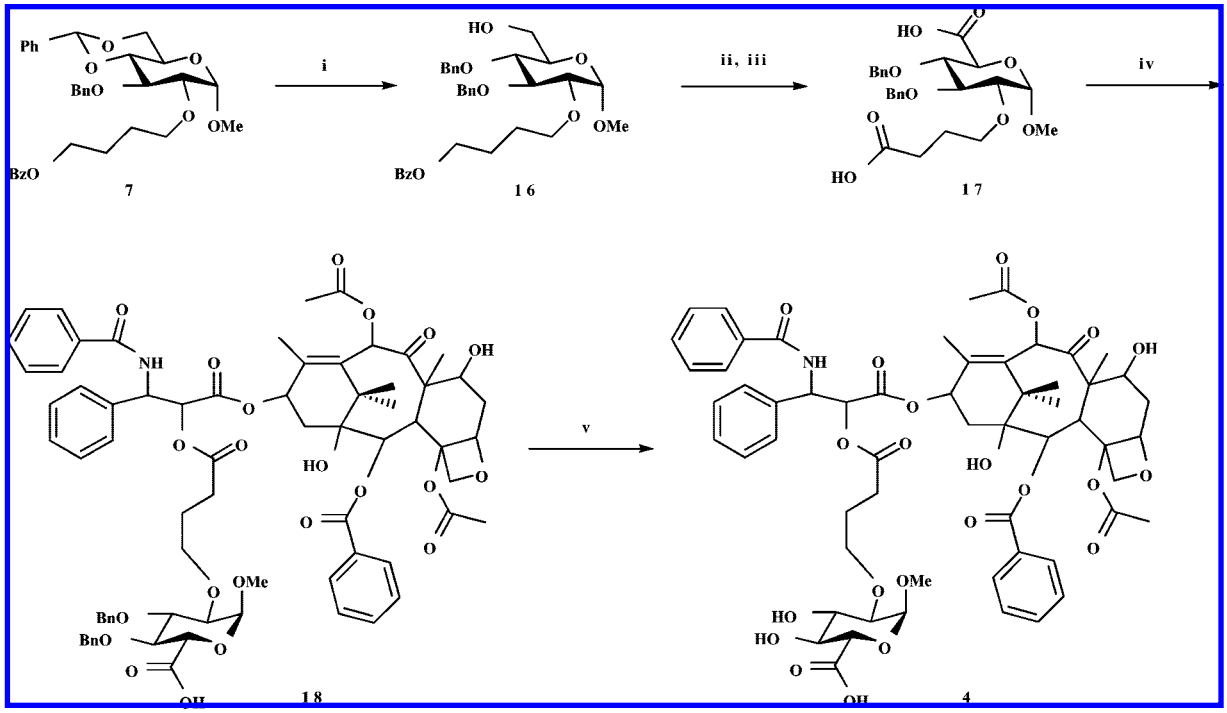

[a] Reagents and conditions: (i) $AlCl_3$, NEt_3BF_3, toluene, 0 °C, 20 min, 62%; (ii) NaOH, MeOH, rt, 2 h; (iii) Jones reagent, rt, 18 h, 2 steps 60%; (iv) paclitaxel, DCC, DMAP, THF, rt, 20 h, 73%; (v) H_2, Pd/C, MeOH, rt, 18 h, 90%.

cells either without prodrug treatment or with treatment of 100 μg/mL paclitaxel.

To study the modified prodrug's delivery into NPC-TW01 cells via GLUTs, we treated NPC-TW01 cells with a glucose transporter inhibitor, phloretin.[36−38] This inhibitor blocks the transporter and is not affect to the cell viability of NPC-TW01 cells (Figure S6, Supporting Information). We were able to observe its influence on the prodrug uptake. The prodrug uptake in NPC-TW01 cells with and without phloretin treatment was determined by RP-HPLC and the results showed that phloretin can block the prodrug delivery into NPC-TW01 cells (Figures S7 and S8, Supporting Information). In addition, the internalization of fluorescently labeled prodrug **1** was detected under fluorescence microscopy. The fluorescence microscopy analysis revealed that inhibitor-treated NPC-TW01 cells could only take up a tiny amount of the glucose-conjugated prodrug **1**, possibly due to passive diffusion (Figure 4). These results suggest that the delivery of the glucose-based paclitaxel prodrug is glucose

Scheme 5. Synthesis of Fluorescently Labeled Prodrug **1**[a]

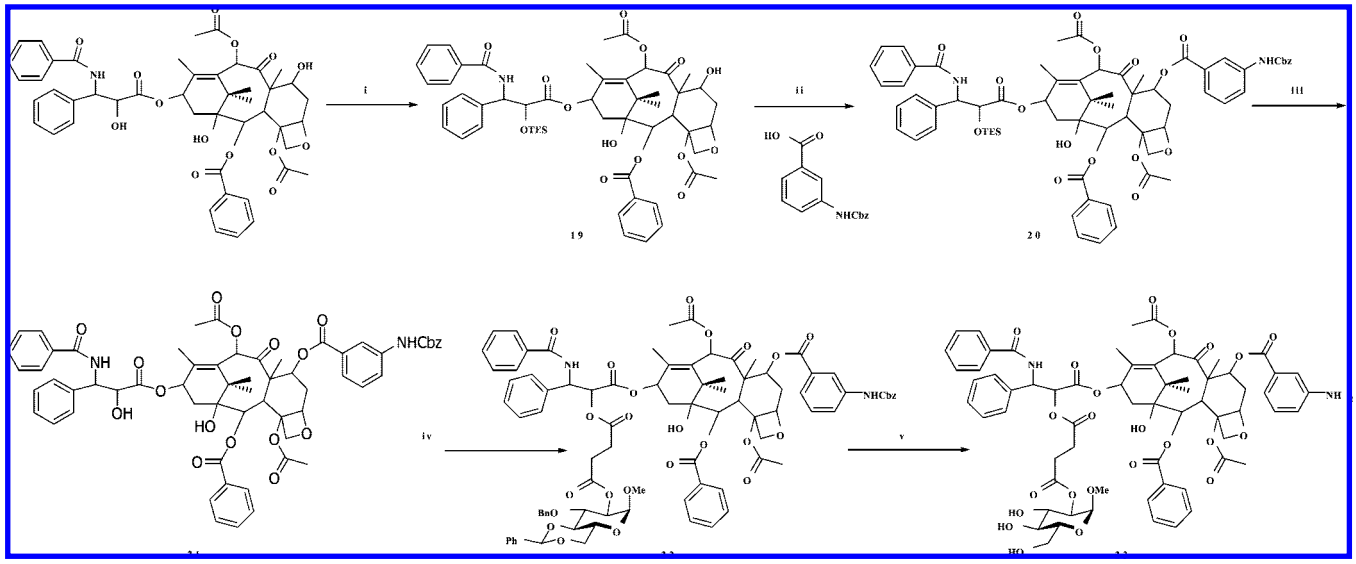

[a] Reagents and conditions: (i) TESCl, Pyr, rt, 3 h, 84%; (ii) DCC, DMAP, THF, rt, 18 h, 46%; (iii) TBAF, THF, rt, 2 h, 100%; (iv) **5**, DCC, DMAP, THF, rt, 18 h, 85%; (v) H_2, Pd/C, MeOH, rt, 12 h, 97%.

Table 1. Cytotoxic Activities of Paclitaxel and Four Glycan-Based Paclitaxel Prodrugs against Seven Cancer Cell Lines and Two Normal Cell Lines[a]

		GLUT protein expression[c]			IC$_{50}$ (μM)[e]				
cells	GLUTs[b]	cancer tissues	normal tissues	GLUT gene expression[d]	Paclitaxel	**1**	**2**	**3**	**4**
1. NCI-H838 lung adenocarcinoma	GLUT-1[26]	7/12	weak	0.843	0.026	0.082	0.374	0.267	0.181
	GLUT-4	−	−	0.572					
2. Hep-3B hepatocellular carcinoma	GLUT-1[27]	2/12	weak	0.764	7.26	100	>100	>100	>100
	GLUT-4	−	−	0.772					
3. A498 renal carcinoma	GLUT-1[28]	4/12	weak	0.973	8.81	>100	>100	>100	>100
	GLUT-4	−	−	0.189					
4. MES-SA uterine carcinoma	GLUT-1[29]	10/12	moderate	0.902	0.008	0.082	0.174	0.095	0.201
	GLUT-4	−	−	0.332					
5. HCT-116 colon carcinoma	GLUT-1[30]	7/12	strong	0.961	0.061	0.100	0.480	0.452	0.469
	GLUT-4	−	−	0.159					
6. NPC-TW01 nasopharyngeal carcinoma	GLUT-1[31]	NS	−	0.867	0.006	0.025	0.078	0.067	0.067
	GLUT-4	−	−	0.115					
7. MKN-45 gastric carcinoma	GLUT-1[32]	1/12	moderate	0.910	89.06	>100	>100	>100	>100
	GLUT-4[32]	NS	NS	0.036					
8. HUV-EC-C human umbilical cord endothelial cell line	GLUT-1[33]	NS	NS	0.252	5.14	>100	>100	>100	44
	GLUT-4	−	−	0.000					
9. CHO-K1 Chinese hamster ovary cell line	GLUT-1[34]	6/12	negative	0.398	15.99	>100	>100	>100	24
	GLUT-3[34]	3/12	negative	−					
	GLUT-4[35]	NS	NS	0.354					

[a] Also Indicated is the Relative Expression Levels of GLUT Proteins among the Tissues and GLUT Genes among the Tested Cell Lines. Symbol: NS, non-observed; -, no expression. [b] GLUTs, according to references of GLUTs in each cell line in the first column. [c] The GLUT protein expression levels in human cancer and normal tissues were searched on the Human Protein Atlas (HPA) database (http://www.proteinatlas.org/), which detected using immunohistochemistry. The GLUT protein expression showed the number of positive staining per 12 tissues in cancer and the evaluated value in normal tissues, respectively. [d] GLUT gene expression level was determined in 9 cell lines by RT-PCR and also shows in Figure S5, Supporting Information. [e] The value of IC$_{50}$ (50% inhibition concentration) represents the means of at least three independent experiments with SD less than 10%.

transporter-dependent. Thus, a paclitaxel-derived prodrug conjugated with glucose as a carrier can be selectively delivered to cancer cells which overexpress GLUTs. This approach can minimize the side effects of prodrugs on normal tissues.

Confocal Microscopy Analysis of NPC-TW01 Cells Treated with Prodrugs. Paclitaxel is an anticancer drug that inhibits mitosis. This drug stabilizes microtubule polymers and leads to G2/M phase cell cycle arrest and subsequent cell death. We designed the carbohydrate modifications to block the active site of paclitaxel (2′-OH) in our prodrugs, leading them to temporarily lose their microtubule-stabilizing ability. We assumed that paclitaxel was released after carbohydrate cleavage and linker autocatalysis inside the cells. To prove that these prodrugs caused cell death by the same biological mechanism as paclitaxel, we investigated the morphological changes in tubulin in NPC-TW01 cells that were treated with paclitaxel or prodrugs (1 μM). These changes were visualized by indirect immunofluorescent staining using a β-tubulin antibody (Figure 5a−f). After 24 h treatment, many microtubules were aggregated around the nuclei of these NPC-TW01 cells. We also observed the relative cellular location of prodrug **1** and tubulin by treating cells with fluorescently labeled prodrug **1** and immunostaining

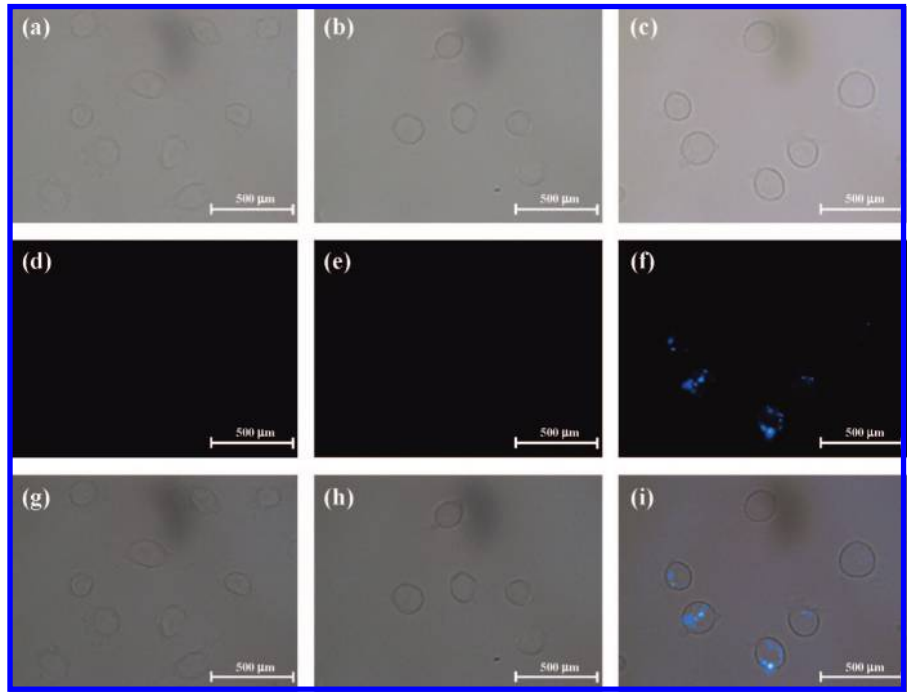

Figure 2. Internalization of prodrug **1** into NPC-TW01 cells under fluorescence microscopy. Fluorescence microscopy images represent the NPC-TW01 cells in the absence of any drugs (a, d, and g), paclitaxel (b, e, and h), and fluorescently labeled prodrug **1** (c, f, and i). Panels a−c are observed under white light, panels d−f are observed under fluorescence, and panels g−i are the merged images. After cell treatment with fluorescently labeled prodrug **1** for 5 h, the fluorescent drug was observed in the plasma regions of cells under fluorescent microscopy.

them for tubulin. The results showed that prodrug **1** is colocalized with tubulin. Thus, we demonstrated that the prodrug was internalized into cells and exhibited the same mechanism of cell death as paclitaxel. However, after prodrug treatment for 24 h, there were still small microtubule bundles in the cytoplasm. Compared with paclitaxel alone, it is possible that the prodrugs may need more time to release paclitaxel and inhibit microtubule disassembly. Thus, the degree of microtubule aggregation induced by prodrugs may be weaker than that induced by paclitaxel. In addition, the chromosomal condensation, which is a special characteristic of apoptotic cells, was dispersed around the nuclei of viable NPC-TW01 cells. However, the chromosomes of viable cells treated with paclitaxel or prodrugs were condensed into fragments (Figure 5g−l). These results indicate that these prodrugs can inhibit microtubule disassembly and induce cell death through apoptosis.

Discussion

Specific characteristics of cancer cells, such as high GLUT expression levels, fast glucose uptake, high energy consumption, and intracellular digestion,[8,39] can be exploited to develop novel prodrugs that overcome certain limitations of anticancer agents, like low solubility and low selectivity. In our previous report, prodrug **1** was synthesized using a glucose−ester conjugate, and its cytotoxicity against various cell lines was examined.[6] However, the mechanism of drug targeting was unknown, and it was not clear if the bulky structure of paclitaxel could pass through the GLUT. To develop a practical synthetic method for glycan-based paclitaxel prodrugs, the synthesis of prodrug **1** was slightly modified as shown in Scheme 1. The total yield was increased to 45%, compared with the previously reported total yield of 25%. In addition, the current study avoided the low yield (27%) synthetic step in coupling 2′-succinyl paclitaxel with 3-*O*-benzyl-4,6-*O*-benzylidene methyl-D-glucopyranoside (Scheme 2). The reasons for using the different glycans and linkages were the following: (i) the conjugated glucose at 2′-position of paclitaxel facilitated the delivery of paclitaxel to specific cancer cells via GLUTs; (ii) the glucuronic acid analogue can be digested by β-glucuronidase and then release the paclitaxel into target cells; (iii) the glucose and glucuronic acid improve paclitaxel's solubility; and (iv) the ester and ether linkages are easily hydrolyzed and readily release paclitaxel into cells. Therefore, we investigated the physiological changes of targeted cancer cells treated with these novel glycan-based paclitaxel prodrugs, which can be transported into cancer cells quickly through GLUTs and release paclitaxel into specific target cells.

According to previous studies, the C2′-hydroxyl group is critical to the biological activity of paclitaxel, and modifications at this position reduce the cytotoxicity of the compound dramatically.[11,40,41] We examined the cytotoxic effects of modifying the 2′-position of paclitaxel using succinic acid as a linker between paclitaxel and glucose. The results showed a concentration-dependent inhibition of MCF-7 cancer cell growth with the IC_{50} of 25 ng/mL (Figure 6). Although modifying the 2′-hydroxyl group of paclitaxel with succinic acid appeared to reduce the toxicity of paclitaxel to cancer cells, this linker preserved the activity of paclitaxel and could be used for further conjugation with 2′-glucopyranose. Thus, we chose to modify this position in the prodrugs. This position was blocked by conjugation with a four-carbon spacer between paclitaxel and the target glycan. Prodrugs **1** and **2** were glucose-conjugated paclitaxel derivatives that were apparently internalized into cancer cells through GLUTs on cell membrane surfaces. In contrast, **3** and **4** are glucuronic acid-conjugated paclitaxels, in which the glucose analogue apparently allows the prodrug to diffuse into cells. If this is the case, the cytotoxicity values of prodrugs **1** and **2** should be better than those of prodrugs **3** and **4**. However, the cytotoxicity values of prodrugs **3** and **4** were higher than that of prodrug **2**. These results suggest that the

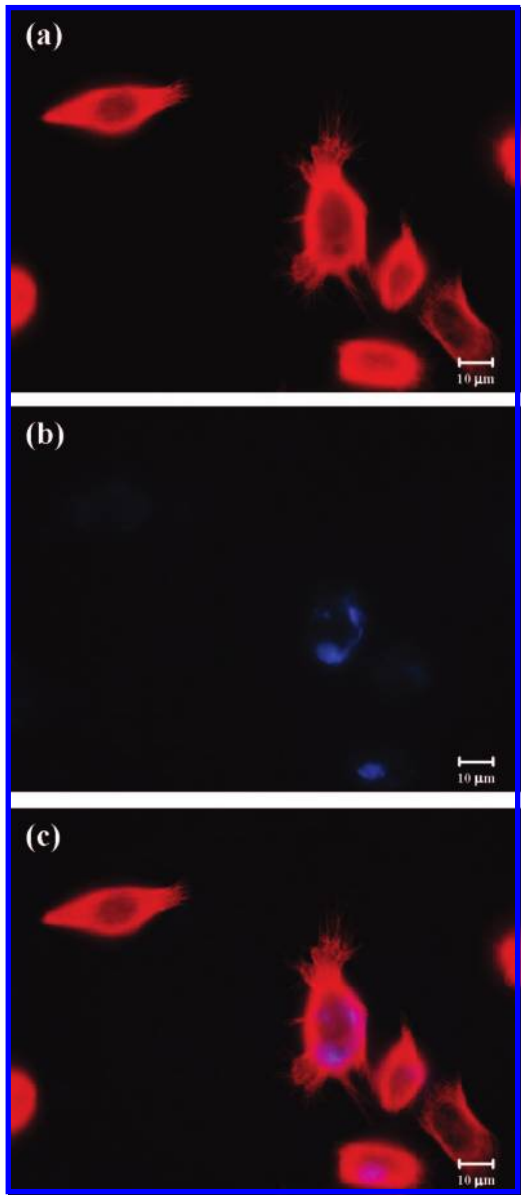

Figure 3. Colocalization of prodrug **1** and tubulin in NPC-TW01 cells under fluorescence microcopy. Fluorescence microscopy images represent the relative position of fluorescence-labeled prodrug **1** and tubluin. The distributions of tubulin and fluorescence-labeled prodrug **1** are represented in panels a and b, respectively. Panel c is the merged images. These images show the colocalization of prodrug **1** and tubulin.

glucuronic acid conjugate, which has a similar structure to glucose, may be transported via GLUTs.

In addition, another difference between prodrugs **1** and **3**, as compared to prodrugs **2** and **4**, was the type of linkage with glucose or glucuronic acid. The glycan linkage of prodrugs **1** and **3** was an ester bond, while the glycan linkage of prodrugs **2** and **4** was an ether bond. The ether bond in prodrugs **2** and **4** was designed to imitate the glycosidic bond and enhance the rates of enzyme-cleavage. We hypothesized that the order of cytotoxicity among the prodrugs should be **2** > **1** > **4** > **3**, but the experimental results showed the order of cytoxicity was **1** > **2** > **3** > **4**. The labile property of the ester bond may be the reason for the greater cytotoxicity of prodrug **1**.

To investigate the possibility of prodrug cleavage outside cells, the NPC-TW01 cells were cultured in the medium with and without FBS (serum free medium) and treated with prodrug **1**. After 4, 8, and 24 h, the quantification of prodrug **1** in the medium, serum free medium and cell cultured medium was analyzed by RP-HPLC. The RP-HPLC analysis revealed that the prodrug **1** was not cleaved by any extracellular enzymes, for example, β-glucuronidase from FBS, outside the cells (Figures S9 and S10, Supporting Information). The prodrug uptake and the release paclitaxel were detected at 8 h and significantly increased at 24 h. We suggest that the prodrug may be cleaved by the intracellular enzymes, in which the β-glucuronidase may be secreted from other organelles inside the cells.

Furthermore, the drug localization in cancer cells was examined with fluorescent microscopy. The fluorescently labeled prodrug **1** was synthesized by conjugation of a chromophore, *m*-aminobenzoic group, at the 7′-position of paclitaxel. Here, the C7′-hydroxyl group was not involved in paclitaxel's modification, but it is a good future candidate for fluorescent labeling. After treatment for 5 h, light blue fluorescence appeared in the cytoplasm of NPC-TW01 cells. This indicated that prodrug **1** was rapidly transported into cancer cells. In addition, the tubulin distribution and chromosome morphology were examined by indirect immunofluorescent staining with confocal microscopy. The tubulin in untreated cells appeared as dispersed bundled structures. After treatment with paclitaxel and the prodrugs, the tubulin structure in the NPC-TW01 cells was aggregated around the nuclei. These results indicate that the free paclitaxel can be released from the prodrugs and affect targeted cells. However, the extent of tubulin aggregation during prodrug treatment was not as strong as that seen with paclitaxel treatment. This difference in tubulin aggregation may reflect the relative release efficiency of paclitaxel. Moreover, changes in chromosome condensation were observed in cells treated with prodrugs. These results indicate that the prodrugs may lead to cell cycle arrest or apoptosis of cancer cells. In future studies, we plan to study the precise mechanisms of drug delivery, the pharmacokinetics of different prodrugs, and their therapeutic applications.

Conclusions

In this study, four glycan-based paclitaxel prodrugs were synthesized using either ester or ether bonds as linkers between 2′-paclitaxel and glucose or glucuronic acid. These prodrugs are not only more water soluble than paclitaxel, they also have enhanced delivery to specifically targeted cells. In addition, prodrug **1** showed the most cytotoxicity against cancer cells and could induce tubulin aggregation and chromosomal condensation in NPC-TW01 cells, which could lead to cell cycle arrest or apoptosis of cancer cells. This study proved that the expression of GLUTs not only contributes to glucose uptake, but also allows for the uptake of glucose derivatives with bulky parent structures such as paclitaxel. However, it is also depended on the selective cytotoxicity of prodrug against each type of cancer cells. Therefore, these prodrugs may potentially be used for further therapeutic applications, and the design of prodrugs using a glucose conjugate with an ester linkage may be used as a technique for the targeted delivery of other drugs.

Experimental Section

Materials. Paclitaxel was purchased from Apin Chemical Ltd. (Oxford, U.K.). **C14** was obtained from CNH Technologies, Inc. (Woburn, MA). Succinic anhydride, palladium on 10% activated carbon, 1,4-butandiol, benzoyl chloride, pyridinum dichromate (PDC), chromium(III) oxide, aluminum chloride, boran-trimethylamine, chlorotriethylsolane, tetrabutyl-ammonium iodide, and sodium hydroxide were purchased from Acros Organics (Springfield, NJ). High Pure RNA Isolation kit was purchased from Roche

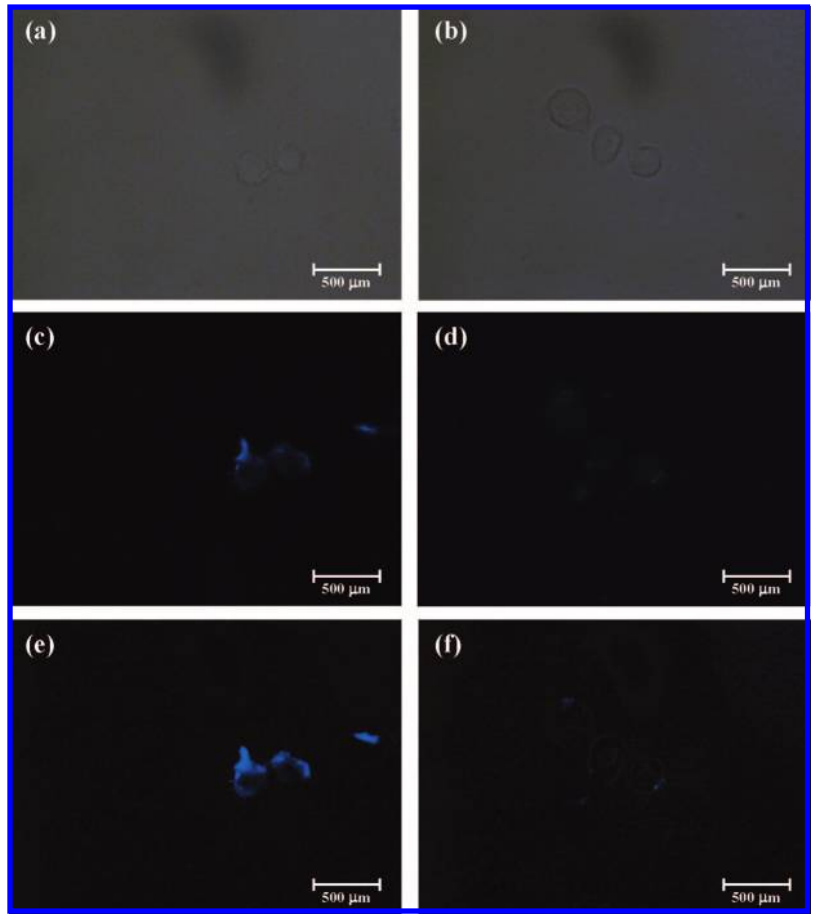

Figure 4. Inhibition of phloretin on internalization of prodrug **1** into NPC-TW01 cells under fluorescence microscopy. Fluorescence microscopy images represent the NPC-TW01 cells treated with fluorescence-labeled prodrug **1** in the absence (a, c, and e) or presence (b, d, and f) of phloretin. Panels a and b are observed under white light, panels c and d are observed under fluorescence, and panels e and f are the merged images.

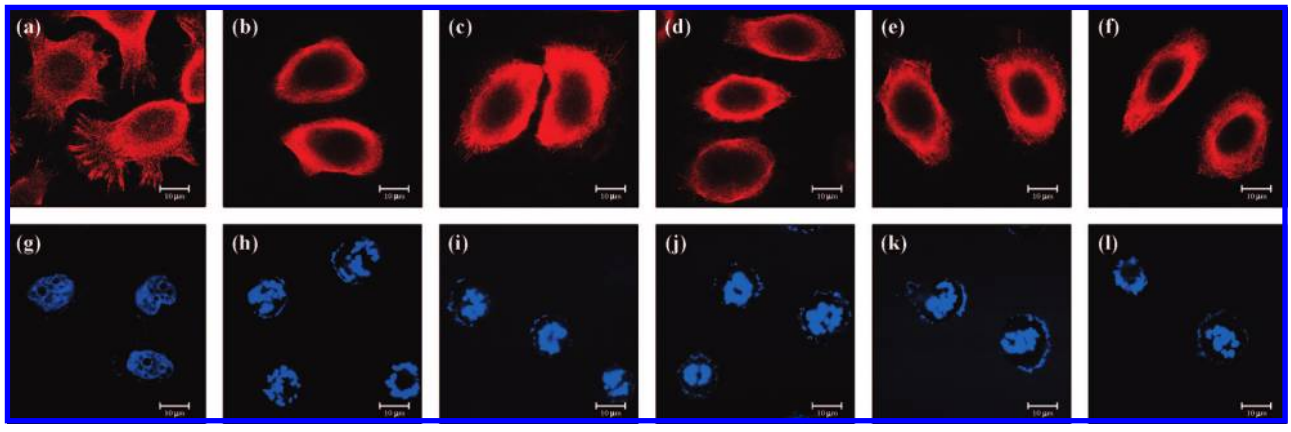

Figure 5. Morphological observations of NPC-TW01 cells treated with paclitaxel and glycan-based paclitaxel prodrugs under confocal microscopy. Confocal microscopy images represent the tubulin distribution (a−f) and the chromosome morphology (g−l) of NPC-TW01 cell. These images were taken in the absence of both drugs (a and g), and in the presence of either 1 μM paclitaxel (b and h), prodrug **1** (c and i), prodrug **2** (d and j), prodrug **3** (e and k), or prodrug **4** (f and l). Nuclei were stained with Hoechst 33258 dye. The chromosomal aggregation in cells treated with paclitaxel and prodrugs was detected under confocal microscopy.

(Mannheim, Germany). Sodium hydride was obtained from Alfa Aesar (Ward Hill, MA). Dicyclohexylcarbodiimide (DCC) was purchased from Fluka Chemie AG (Buchs, Switzerland). 4-Dimethylaminopyridine (DMAP) was obtained from Aldrich Chemical Co. (Milwaukee, WI). 3-Aminobenzoic acid was purchased from Merck (Darmstadt, Germany). NCI-H838 (lung), MCF-7 (breast), Hep-3B (liver), A-498 (kidney), HCT-116 (colon), MES-SA (uterus), NPC-TW01 (nasopharynx), and MKN-45 (stomach) cancer cell lines were obtained from American Type Culture Collection (ATCC; Rockville, MD). Phloretin (3-[4-hydroxyphenyl-]-1-[2,4,6-trihydroxyphenyl]-1-propanone), RPMI-1640, Minimum Essential Medium Eagle (MEME), McCoy's 5A, Dulbecco's Modified Eagle's Medium (DMEM), Ham's F12K medium, and antibiotics were purchased from Sigma (St. Louis, MO). Fetal bovine serum (FBS), glutamine and ProLong Gold antifade reagent were purchased from Invitrogen (Carlsbad, CA).

Synthesis of Prodrugs 1−4. Prodrugs **1**, **2**, **3**, and **4** were synthesized by following the procedures described in Schemes 1, 2, 3, and 4, respectively.

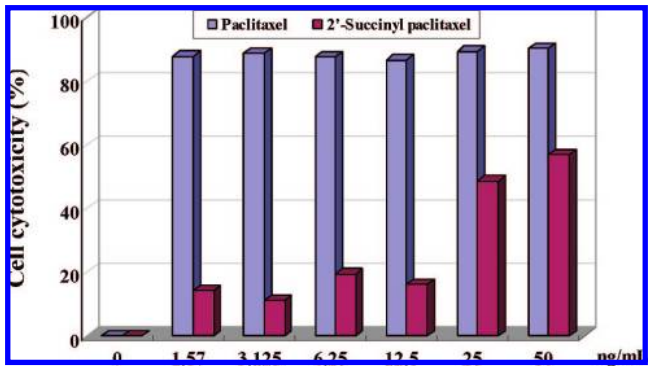

Figure 6. Cell cytotoxicity of paclitaxel and 2′-succinyl paclitaxel against MCF-7 cells at 72 h. The concentrations of paclitaxel and 2′-succinyl paclitaxel used were 1.57, 3.125, 6.25, 12.5, 25, and 50 ng/mL. The cell proliferation was examined by the MTT assay.

Succinic Acid Mono-(8-benzyloxy-6-methoxy-2-phenyl-hexahydro-pyrano[3,2-*d*][1,3]dioxin-7-yl) Ester (5). The succinic acid mono-(8-benzyloxy-6-methoxy-2-phenyl-hexahydro-pyrano[3,2-*d*][1,3]dioxin-7-yl) ester (**5**) was synthesized as described below. Briefly, the mixture of succinic anhydride (1.345 g, 13.45 mmol), DMAP (33 mg, 0.27 mmol) and C14 (1.0 g, 2.69 mmol) in Pyr (15 mL) was stirred at room temperature for 12 h. After quenching with brine (15 mL), the mixture was extracted with EtOAc (15 mL × 3), dried over $MgSO_4$, and concentrated. The residue was purified by silica gel chromatography (CH_2Cl_2/MeOH = 20/1) and dried under vacuum to produce a white solid **5** (898 mg, 71%). ^{1}H NMR (400 MHz, $CDCl_3$) δ 7.25−7.50 (m, 10 H), 5.59 (s, 1 H, H7), 4.86−4.93 (m, 3 H, H1, H2, and −OCH_2Ph), 4.70 (d, 1 H, J = 11.8 Hz, -OCH_2Ph), 4.30 (dd, 1 H, J = 9.9, 4.4 Hz, H6), 4.01−4.07 (m, 1 H, H3), 3.85 (ddd, 1 H, J = 9.9, 4.4 Hz, H5), 3.78 (t, 1 H, J = 9.9 Hz, H6), 3.71 (t, 1 H. J = 9.5 Hz, H4), 3.38 (s, 3 H, -OCH_3), 2.57−2.70 (m, 4 H, Hb and Hc); ^{13}C NMR (100 Hz, $CDCl_3$) δ 176.71 (C, Ca or Cd), 171.60 (C, C1′ or C4′), 137.25 and 138.44 (C, aromatic), 126.02−129.5 (CH, aromatic), 101.36 (CH, C7), 97.67 (CH, C1), 82.03 (CH, C4), 76.09 (CH, C3), 74.78 (CH_2, -OCH_2Ph), 73.26 (CH, C2), 68.92 (CH_2, C6), 62.27 (CH, C5), 55.30 (CH_3, OCH_3), 28.76 (CH_2, Cb or *Cc*), 28.62 (CH_2, Cb or *Cc*).

C15 (6). C15 (**6**) was synthesized as described below. Briefly, the mixture of paclitaxel (50 mg, 0.06 mmol), DCC (36 mg, 0.18 mmol), and DMAP (3 mg, 0.02 mmol) in THF (2 mL) was added into a solution of **5** (55 mg, 0.12 mmol) in THF (2 mL). After stirring at room temperature for 20 h, and subsequent concentration, the residue was purified by silica gel chromatography (EtOAc/Hex = 4/1) and dried under vacuum to produce a white solid **6** (66.8 mg, 87.3%). ^{1}H NMR (400 MHz, $CDCl_3$) δ 7.20−8.16 (m, 25H, aromatic), 7.01 (d, 1H, J = 9.1 Hz, NH), 6.22−6.28 (m, 2H, H10 and H13), 5.98 (dd, 1H, J = 9.1, 3 Hz, H3′), 5.69 (d, 1H, J = 7.0 Hz, H2), 5.58 (s, 1H, H7″), 5.49 (d, 1H, J = 3.0 Hz, H2′), 4.97 (m, 1H, H5), 4.80−4.87 (m, 3H, H1″ and H2″ and −OCH_2Ph), 4.65 (d, 1H, J = 11.9 Hz, -OCH_2Ph), 4.44 (dd, 1H, J = 7.3, 6.6 Hz, 7H), 4.27−4.33 (m, 2H, H20 and H6″), 4.20 (d, 1H, J = 8.4 Hz, H_20), 3.99 (t, 1H, J = 9.2 Hz, H3″), 3.75−3.86 (m, 2H, H3 and H5″ and H6″), 3.64 (t, 1H, J = 9.2 Hz, H4″), 3.34 (s, 3H, -OCH_3), 2.52−2.78 (m, 5H, Hb and Hc and H6′), 2.44 (s, 3H, 4-OAc), 2.34−2.41 (m, 1H, H14′), 2.23 (s, 3H, 10-OAc), 2.14−2.20 (m, 1H, H14), 1.92 (s, 3H, H18), 1.85−1.90 (m, 1H, H6), 1.68 (s, 3H, H19), 1.14 (s, 3H, H15 or H16), 0.98 (s, 3H, H15 or H16); ^{13}C NMR (100 MHz, $CDCl_3$) δ 203.80 (C, C9), 171.43 (C, -COOH), 171.23 (C, -COOH), 171.02 (C, -COOH), 169.79 (C, -COOH), 167.88 (C, -COOH), 167.15 (C, -COOH), 167.03 (C, -COOH), 142.72 (C or CH, aromatic or C11 or C12), 138.41 (C or CH, aromatic or C11 or C12), 137.19 (C or CH, aromatic or C11 or C12), 136.93 (C or CH, aromatic or C11 or C12), 133.66 (C or CH, aromatic or C11 or C12), 133.57 (C or CH, aromatic or C11 or C12), 132.79 (C or CH, aromatic or C11 or C12), 131.99 (C or CH, aromatic or C11 or C12), 130.23 (C or CH, aromatic or C11 or C12), 129.10 (C or CH, aromatic or C11 or C12), 129.02 (C or CH, aromatic or C11 or C12), 128.69 (C or CH, aromatic or C11 or C12), 128.48 (C or CH, aromatic or C11 or C12), 128.26 (C or CH, aromatic or C11 or C12), 127.65 (C or CH, aromatic or C11 or C12), 127.21 (C or CH, aromatic or C11 or C12), 126.53 (C or CH, aromatic or C11 or C12), 126.00 (C or CH, aromatic or C11 or C12), 101.36 (CH, C7″), 97.54 (CH, C1″), 84.44 (CH, C5), 82.09 (CH, C4″), 81.05 (C, C4), 79.12 (C, C1), 75.96 (CH, C3″), 75.58 (CH, C10), 75.09 (CH, C2), 74.73 (CH_2, -CH_2Ph), 74.25 (CH, C2′), 73.14 (CH, C2″), 72.11 (CH, C7), 71.86 (CH, C13), 68.90 (CH_2, C6″), 62.25 (CH, C5″), 58.51 (C, C8), 55.20 (CH_3, -OCH_3), 52.71 (CH, C3′), 45.53 (CH, C3), 43.17 (C, C15), 35.53 (CH_2, C6 or C14), 28.99 (CH_2, Cb or *Cc*), 28.88 (CH_2, Cb or *Cc*), 26.79 (CH_3, C16), 22.66 (CH_3, 4-$OCOCH_3$), 22.13 (CH_3, C17), 20.81 (CH_3, 10-$OCOCH_3$), 14.76 (CH_3, C18), 9.58 (CH_3, C19); *m/z* 1308.5008 $(M + H)^+$, 1330.4829 $(M + Na)^+$.

Prodrug 1 (1). The mixture of **6** (46 mg, 0.035 mmol) and Pd/C (25 mg) in MeOH (4 mL) was stirred at room temperature in hydrogen for 12 h. After filtering by celite and silica gel, the residue was concentrated and recrystallized to give a white solid of prodrug **1** (37 mg, 93.1%). ^{1}H NMR (400 MHz, $CDCl_3$) δ 7.29−8.13 (m, 15H, aromatic), 7.13 (d, 1H, J = 9.0 Hz, NH), 6.30 (s, 1H, H10), 6.17 (t, 1H, J = 8.7 Hz, H13), 5.92 (dd, 1H, J = 9.0, 4.2 Hz, H3′), 5.66 (d, 1H, J = 7.0 Hz, H2), 5.48 (d, 1H, J = 4.2 Hz, H2′), 4.96 (m, 1H, H5), 4.82 (d, 1H, J = 3.6 Hz, H1″), 4.67 (dd, 1H, J = 9.7, 3.6 Hz, H2″), 4.41 (m, 1H, H7), 4.30 (d, 1H, J = 8.5 Hz, H20), 4.13 (d, 1H, J = 8.5 Hz, H_20), 3.92 (ddd, 1H, J = 9.7, 9.7, 4.4 Hz, H3″), 3.80−3.85 (m, 2H, H6″), 3.77 (d, 1H, J = 7.0 Hz, H3), 3.52−3.63 (m, 2H, H4″ and H5″), 3.35 (s, 3H, -OCH_3), 3.24 (d, 1H, J = 4.4 Hz, 3″-OH), 3.18 (d, 1H, J = 3.0 Hz, 4″-OH), 2.64−2.76 (m, 5H, Hb, Hc, and 7-OH), 2.50−2.57 (m, 1H, H6), 2.41 (s, 3H, 4-OAc), 2.24−2.34 (m, 2H, H14 and 6″-OH), 2.22 (s, 3H, 10-OAc), 2.04−2.10 (m, 1H, H14), 1.84−1.90 (m, 5H, H6, H10, and H18), 1.67 (s, 3H, H19), 1.21 (s, 3H, H15 or H16), 1.13 (s, 3H, H15 or H16); ^{13}C NMR (100 MHz, $CDCl_3$) δ 203.69 (C, C9), 171.84 (C, Ca), 171.68 (C, Cd), 171.25 (C, 4 or 10-$OCOCH_3$), 170.00 (C, 4 or 10-$OCOCH_3$), 168.11 (C, C1′), 167.27 (C, 3′-$NHCOC_6H_5$), 166.97 (C, 2-$OCOC_6H_5$), 142.45 (C, C12), 136.74 (C, aromatic or C11), 133.68 (CH, aromatic or C11), 132.86 (C, aromatic or C11), 132.01 (CH, aromatic or C11), 130.19 (C, aromatic or C11), 129.10 (CH, aromatic or C11), 128.68 (CH, aromatic or C11), 127.21 (CH, aromatic or C11), 126.73 (CH, aromatic or C11), 97.00 (CH, C1″), 84.38 (CH, C5), 81.12 (C, C4), 79.06 (C, C1), 75.57 (CH, C10), 75.02 (CH, C2), 74.52 (CH, C2′), 73.70 (CH, C2″), 71.96 (CH, C7 and C3″), 71.63 (CH, C13), 70.91 (CH, C4″ or C5″), 70.72 (CH, C4″ or C5″), 62.08 (CH_2, C6″), 58.41 (C, C8), 55.15 (CH_3, -OCH_3), 52.97 (CH, C3′), 45.71 (CH, C3), 43.13 (C, C15), 35.60 (CH, C6 or C14), 35.39 (CH, C6 or C14), 29.08 (CH_2, Cb and *Cc*), 26.73 (CH_3, C17), 22.62 (CH_3, 4-$OCOCH_3$), 22.01 (CH_3, C16), 20.82 (CH_3, 10-$OCOCH_3$), 14.79 (CH_2 or CH_3, C18), 14.08 (CH_2 or CH_3, C6 or C18), 9.61 (CH_3, C19); *m/z* 1130.4227 $(M+H)^+$, 1152.4047 $(M+Na)^+$.

Benzoic Acid 4-(8-Benzyloxy-6-methoxy-2-phenyl-hexahydro-pyrano[3,2-*d*][1,3] dioxin-7-yloxy)-butyl Ester (7). The benzoic acid 4-(8-benzyloxy-6-methoxy-2-phenyl-hexahydro-pyrano[3,2-*d*][1,3]dioxin-7-yloxy)-butyl ester (**7**) was synthesized as described below. Briefly, the mixture of C14 (1000 mg, 2.69 mmol), benzoic acid 4-bromo-butyl ester (1380 mg, 5.37 mmol), sodium hydride (300 mg, 8.0 mmol), and TBAI in DMF (15 mL) was stirred at room temperature for 36 h. After quenching with water (10 mL), the mixture was extracted with EtOAc, dried over $MgSO_4$ and concentrated. The residue was purified by silica gel chromatography (EtOAc/Hex = 1/2) and dried under vacuum to produce a white solid, **9** (1080 mg, 73.3%). ^{1}H NMR (400 MHz, $CDCl_3$) δ 7.25−8.07 (m, 15H, aromatic), 5.59 (s, 1H, H7), 4.81−4.93 (m, 3H, H1 and −OCH_2Ph), 4.30−4.36 (m, 3H, H6 and Hd), 4.00 (t, 1H, J = 9.3 Hz, H3), 3.86 (ddd, 1H, J = 9.3, 9.3, 4.6 Hz, H5), 3.74−3.79 (m, 3H, H6 and H1a), 3.60−3.65 (m, 3H, H4 and Hd), 3.50 (dd, 1H, J = 9.3, 3.6 Hz, H2), 3.46 (s, 3H, -OCH_3), 1.80−1.88 (m, 4H, Hb and Hc); ^{13}C NMR (100 Hz, $CDCl_3$) δ 166.6 (C, -OCOPh), 138.73 (C, aromatic), 137.42 (C, aromatic), 132.90 (CH,

aromatic), 130.38 (CH, aromatic), 129.57 (CH, aromatic), 128.93 (CH, aromatic), 128.36 (CH, aromatic), 128.29 (CH, aromatic), 128.24 (CH, aromatic), 127.91 (CH, aromatic), 127.58 (CH, aromatic), 126.06 (CH, aromatic), 101.27 (CH, C7), 98.87 (CH, C1), 82.14 (CH, C4), 80.50 (CH,C2), 78.39 (CH, C3), 75.28 (CH_2, -OCH_2Ph), 71.39 (CH_2, C6), 69.10 (CH_2, Cd), 64.70 (CH, C5), 62.37 (CH_2, Ca), 55.33 (CH_3, -OCH_3), 26.70 (CH_2, Cb or *Cc*), 25.47 (CH_2, Cb or *Cc*); *m/z* 549.2483 $(M + H)^+$, 571.2302 $(M + Na)^+$.

Prodrug 2 (2). The mixture of **10** (55 mg, 0.044 mmol) and Pd/C (28 mg) in MeOH (4 mL) was stirred at room temperature in hydrogen for 12 h. After filtering by celite and silica gel, the residue was concentrated and recrystallized to give a white solid of prodrug **2** (47 mg, 95%). ^{1}H NMR (400 MHz, $CDCl_3$) δ 7.34−8.15 (m, 15H, aromatic), 7.23 (d, 1H, J = 9.2 Hz, NH), 6.31 (s, 1H, H10), 6.24 (t, 1H, J = 8.5 Hz, H13), 5.99 (dd, 1H, J = 9.2, 3.5 Hz, H3′), 5.69 (d, 1H, J = 7.1 Hz, H2), 5.51 (d, 1H, J = 3.5 Hz, H2′), 4.96−4.99 (m, 1H, H5), 4.79 (d, 1H, J = 3.4 Hz, H1″), 4.44 (dd, 1H, J = 10.6, 6.6 Hz, H7), 4.32 (d, 1H, J = 8.6 Hz, -CH_2Ph), 4.20 (d, 1H, J = 8.6 Hz, -CH_2Ph), 3.75−3.82 (m, 4H, H3, H3″, and H6″), 3.67−3.72 (m, 1H, Ha), 3.54−3.59 (m, 1H, H5″), 3.37−3.49 (m, 5H, H4″, Ha, and −OCH_3), 3.20 (dd, 1H, J = 9.6, 3.4 Hz, H2″), 2.66−2.74 (m, 1H, Hc), 2.52−2.60 (m, 1H, H6), 2.47 (s, 3H, 4-$OCOCH_3$), 2.33−2.44 (m, 2H, H14 and Hc), 2.23 (s, 3H, 10-$OCOCH_3$), 2.14−2.20 (m, 1H, H14), 1.95 (s, 3H, H18), 1.86−1.92 (m, 3H, H6 and Hb), 1.68 (s, 3H, H19), 1.24 (s, 3H, H17), 1.14 (s, 3H, H16); ^{13}C NMR (100 Hz, $CDCl_3$) δ 203.75 (C, C9), 172.76 (C, -COOR), 171.26 (C, -COOR), 169.94 (C, -COOR), 168.46 (C, -COOR), 167.34 (C, -COOR), 166.99 (C, -COOR), 142.54 (C or CH, aromatic or C11 or C12), 136.88 (C or CH, aromatic or C11 or C12), 133.69 (C or CH, aromatic or C11 or C12), 132.85 (C or CH, aromatic or C11 or C12), 132.04 (C or CH, aromatic or C11 or C12), 130.21 (C or CH, aromatic or C11 or C12), 129.18 (C or CH, aromatic or C11 or C12), 129.07 (C or CH, aromatic or C11 or C12), 128.69 (C or CH, aromatic or C11 or C12), 128.48 (C or CH, aromatic or C11 or C12), 127.23 (C or CH, aromatic or C11 or C12), 126.63 (C or CH, aromatic or C11 or C12), 97.35 (CH, C1″), 84.42 (CH, C5), 81.07 (C, C4), 80.04 (CH, C2″), 79.07 (C, C1), 76.40 (CH_2, C20), 75.59 (CH, C10), 75.03 (CH, C2), 74.15 (CH, C2′), 73.00 (CH or CH_2, C3″ or C6″), 71.99 (CH, C7 or C13), 71.92 (CH, C7 or C13), 70.75 (CH, C4″ or C5″), 70.62 (CH, C4″ or C5″), 68.63 (CH_2, Ca), 62.20 (CH or CH_2, C3″ or C6″), 58.41 (C, C8), 55.16 (CH_3, -OCH_3), 52.76 (CH, C3′), 45.67 (CH, C3), 43.16 (C, C15), 35.54 (CH, C6 or C14), 35.60 (CH, C6 or C14), 29.69 (CH_2, *Cc*), 26.78 (CH_3, C17), 24.86 (CH_2, Cb), 22.68 (CH_3, 4-$OCOCH_3$), 22.07 (CH_3, C16), 20.86 (CH_3, 10-$OCOCH_3$), 14.87 (CH_3, C18), 9.64 (CH_3, C19); *m/z* 1138.4254 $(M+Na)^+$.

Benzoic Acid 4,5-Bis-benzyloxy-6-hydroxymethyl-2-methoxy-tetrahydro-pyran-3-yl Ester (12). The mixture of **11** (700 mg, 1.45 mmol) and boran-trimethylamine (635 mg, 8.7 mmol) in toluene (5 mL) was added with aluminum chloride (1.14 g, 8.7 mmol) to ether (5 mL) on ice, and was then stirred on ice for 20 min. After quenching with water, the mixture was extracted with EtOAc, dried over $MgSO_4$, and concentrated. The residue was purified by silica gel chromatography (CH_2Cl_2/MeOH = 40/1) and dried under vacuum to produce a white solid (517 mg, 74.5%). ^{1}H NMR (400 MHz, $CDCl_3$) 7.18−8.08 (m, 15H, aromatic), 5.08 (dd, 1H, J = 9.7, 3.7 Hz, H2), 5.03 (d, 1H, J = 3.7 Hz, H1), 4.90 (d, 1H, J = 11.0 Hz, -CH_2Ph), 4.83 (s, 2H, -CH_2Ph), 4.69 (d, 1H, J = 11.0 Hz, -CH_2Ph), 4.22 (t, 1H, J = 9.7 Hz, H3), 3.68−3.87 (m, 4H, H4, H5, and H6), 3.37 (s, 3H, -OCH_3); ^{13}C NMR (100 Hz, $CDCl_3$) δ 165.98 (C, -COOPh), 138.16 (C, aromatic), 138.03 (C, aromatic), 133.05 (CH, aromatic), 129.84 (CH, aromatic), 129.69 (CH, aromatic), 128.48 (CH, aromatic), 128.45 (CH, aromatic), 128.31 (CH, aromatic), 128.02 (CH, aromatic), 127.86 (CH, aromatic), 127.64 (CH, aromatic), 97.26 (CH, C1), 80.01 (CH, C3), 77.65 (CH, C4 or c5), 75.54 (CH_2, -CH_2Ph), 75.13 (CH_2, -CH_2Ph), 74.20 (CH, C2), 70.87 (CH, C4 or C5), 61.79 (CH_2, C6), 55.22 (CH_3, -OCH_3); *m/z* 479.2064 $(M + H)^+$, 501.1884 $(M + Na)^+$.

3,4-Bis-benzyloxy-5-hydroxy-6-methoxy-tetrahydro-pyran-2-carboxylic Acid Benzyl Ester (13). A solution of **12** (500 mg, 1.05 mmol) in acetone (5 mL) was added with Jones reagent (0.43 M CrO_3 in H_2SO_4, 7.3 mL) on ice. The mixture was stirred at room temperature for 18 h, quenched with water (10 mL), extracted with EtOAc (100 mL × 2), and dried over $MgSO_4$. The crude product was added to 1% NaOH in MeOH and stirred at room temperature for 4 h. The pH of the mixture was adjusted to 2−4 by addition of 0.1 M H_2SO_4. The mixture was extracted with $CHCl_3$ (100 mL × 2), concentrated, and dried under vacuum. The mixture of the crude residue, DCC (336 mg, 1.625 mmol), and DMAP (catalytic amount) in DMF (4 mL) was added to benzyl alcohol (170 μL, 1.625 mmol) and stirred at room temperature for 18 h. After purification by silica gel chromatography (EtOAc/Hex = 1/2), the residue was dried under vacuum to produce a white solid (154 mg, 23%). ^{1}H NMR (400 MHz, $CDCl_3$) δ7.14−7.33 (m, 15H, aromatic), 5.14−5.22 (m, 2H, -CH_2Ph), 4.79−4.85 (m, 3H, H1 and -CH_2Ph), 4.72 (d, 1H, J = 10.8 Hz, -CH_2Ph), 4.48 (d, 1H, J = 10.8 Hz, -CH_2Ph), 4.28−4.30 (m, 1H, H3), 3.75−3.80 (m, 3H, H2, H4, and H5), 3.47 (s, 3H, -OCH_3), 2.27 (d, 1H, J = 7.6 Hz, -OH); ^{13}C NMR (100 Hz, $CDCl_3$) δ 169.39 (C, COOBn), 138.28 (C, aromatic), 137.74 (C, aromatic), 135.05 (C, aromatic), 128.58 (CH, aromatic), 126.46 (CH, aromatic), 128.33 (CH, aromatic), 127.89 (CH, aromatic), 127.77 (CH, aromatic), 99.63 (CH, C1), 81.88 (CH, C2 or C4 or C5), 79.04 (CH, C2 or C4 or C5), 75.25 (CH_2, -CH_2Ph), 74.74 (CH_2, -CH_2Ph), 72.17 (CH, C2 or C4 or C5), 70.87 (CH, C3), 67.33 (CH_2, -CH_2Ph), 55.80 (CH_3, -OCH_3); *m/z* 479.2064 $(M + H)^+$, 501.1884 $(M + Na)^+$.

Prodrug 3 (3). The mixture of **15** (33 mg, 0.023 mmol) and Pd/C (15 mg) in MeOH (2 mL) was stirred at room temperature in hydrogen for 12 h. After filtering by celite and silica gel, the residue was concentrated and recrystallized to give the white solid of prodrug **3** (25 mg, 95%). ^{1}H NMR (400 MHz, $CDCl_3$) δ7.13−8.14 (m, 15H, aromatic), 7.08 (d, 1H, J = 9.2 Hz, NH), 6.29 (s, 1H, H10), 6.20 (t, 1H, J = 8.3 Hz, H13), 5.95 (dd, 1H, J = 9.2, 3.9 Hz, H3′), 5.67 (d, 1H, J = 6.7 Hz, H2), 5.49 (d, 1H, J = 3.9 Hz, H2′), 4.95−4.97 (m, 1H, H5), 4.91 (d, 1H, J = 3.6 Hz, H1″), 4.71 (dd, 1H, J = 9.8, 3.6 Hz, H2″), 4.42 (dd, 1H, J = 11.2, 6.9 Hz, H7), 4.30 (d, 1H, J = 8.4 Hz, H20), 4.19 (d, 1H, J = 8.4 Hz, H20), 4.12 (d, 1H, J = 9.8 Hz, H5″), 3.96 (t, 1H, J = 9.8 Hz, H3″), 3.79 (d, 1H, J = 6.7 Hz, H3), 3.70 (t, 1H, J = 9.8 Hz, H4″), 3.40 (s, 3H, -OCH_3), 2.67−2.79 (m, 4H, Hb and Hc), 2.51−2.57 (m, 1H, H6), 2.42 (s, 3H, 4-$OCOCH_3$), 2.26−2.34 (m, 1H, H14), 2.23 (s, 3H, 10-$OCOCH_3$), 2.04−2.14 (m, 1H, H14), 1.90 (s, 3H, H18), 1.85−1.89 (m, 1H, H6), 1.68 (s, 3H, H19), 1.24 (s, 3H, H16), 1.13 (s, 3H, H17); ^{13}C NMR (100 Hz, $CDCl_3$) δ 203.73 (C, C9), 171.60 (C, -COOR, 171.33 (C, -COOR), 171.22 (C, -COOR), 170.47 (C, -COOR), 169.95 (C, -COOR), 168.14 (C, -COOR), 167.99 (C, -COOR), 167.30 (C, -COOR), 166.98 (C, -COOR), 136.78 (C or CH, aromatic or C11 or C12), 133.61 (C or CH, aromatic or C11 or C12), 132.86 (C or CH, aromatic or C11 or C12), 132.01 (C or CH, aromatic or C11 or C12), 130.20 (C or CH, aromatic or C11 or C12), 129.10 (C or CH, aromatic or C11 or C12), 128.69 (C or CH, aromatic or C11 or C12), 127.21 (C or CH, aromatic or C11 or C12), 126.78 (C or CH, aromatic or C11 or C12), 126.67 (C or CH, aromatic or C11 or C12), 97.31 (CH, C1″), 84.41 (CH, C5), 81.11 (C, C4), 79.09 (C, C1), 75.59 (CH, C10), 75.07 (CH, C2), 74.45 (CH, C2′), 72.82 (CH, C2″), 72.02 (CH, C7 or/and C13 or/and C4″), 71.95 (CH, C7 or/ and C13 or/ and C4″), 70.74 (CH, C3″), 69.73 (CH, C5″), 58.47 (C, C8), 55.78 (CH_3, -OCH_3), 52.82 (CH, C3′), 45.80 (CH,C3), 43.15 (C, C15), 35.54 (CH, C6 and C14), 29.07 (CH_2, Cb and *Cc*), 26.78 (CH_3, C16), 22.63 (CH3, 4-$OCOCH_3$), 22.06 (CH_3, C17), 20.81 (CH3, 10-$OCOCH_3$), 14.76 (CH_3, C18), 9.60 (CH_3, C19); *m/z* 1166.3840 $(M + Na)^+$.

Benzoic Acid 4-(4,5-Bis-benzyloxy-6-hydroxymethyl-2-methoxy-tetrahydro-pyran-3-yloxy)-butyl Ester (16). The mixture of **7** (240 mg, 0.449 mmol) and boran-trimethylamine (196.5 mg, 2.694 mmol) in toluene (2 mL) was added to aluminum chloride (353.8 mg, 2.694 mmol) in ether (2 mL) on ice and stirred on ice for 20 min. After quenching with water, the mixture was extracted with

EtOAc, dried over $MgSO_4$, and concentrated. The residue was purified by silica gel chromatography (EtOAc/Hex = 1/1) and dried under vacuum to produce a white solid (153.1 mg, 62%). ^{1}H NMR (400 MHz, $CDCl_3$) δ 7.25−8.04 (m, 15H, aromatic), 4.81−4.96 (m, 4H, H1 and -CH_2Ph), 4.65 (d, 1H, J = 11.1 Hz, -CH_2Ph), 4.32 (t, 2H, J = 6.0 Hz, Hd), 3.95 (t, 1H, J = 9.2 Hz, H3), 3.63−3.82 (m, 5H, H5, H6, and Ha), 3.54 (t, 1H, J = 9.2 Hz, H4), 3.40−3.43 (m, 4H, H2 and −OCH_3), 1.79−1.85 (m, 4H, Hb and Hc); ^{13}C NMR (100 Hz, $CDCl_3$) δ 166.58 (C, -COPh), 138.75 (C, aromatic), 138.15 (C, aromatic), 132.86 (CH, aromatic), 130.36 (CH, aromatic), 129.54 (CH, aromatic), 128.53 (CH, aromatic), 128.46 (CH, aromatic), 128.36 (CH, aromatic), 128.34 (CH, aromatic), 128.03 (CH, aromatic), 127.84 (CH, aromatic), 127.76 (CH, aromatic), 127.57 (CH, aromatic), 126.94 (CH, aromatic), 97.85 (CH, C1), 81.79 (CH, C3), 81.06 (CH, C2), 75.64 (CH_2, -CH_2Ph), 75.02 (CH_2, -CH_2Ph), 70.83 (C5 or C6), 70.75 (C5 or C6), 64.63 (CH_2, Cd), 61.89 (CH_2, Ca), 55.15 (CH_3, -OCH_3), 26.72 (CH_2, Cb or *Cc*), 25.47 (CH_2, Cb or *Cc*); *m/z* 551.2639 (M + H)$^+$, 573.2459 (M + Na)$^+$.

3,4-Bis-benzyloxy-5-(3-carboxy-propoxy)-6-methoxy-tetrahydro-pyran-2-carboxylic Acid (17). The mixture of **16** (150 mg, 0.28 mmol) and NaOH (17 mg, 0.42 mmol) in MeOH (2 mL) was stirred at room temperature for 2 h. After evaporation of MeOH and subsequent addition of water, the residue was extracted with ether, dried over $MgSO_4$, and concentrated. The crude residue was dissolved in acetone (3 mL), added CrO_3 (0.34 M, 4 mL) in H_2SO_4 on ice, and stirred at room temperature for 18 h. After extraction with $CHCl_3$, the organic layer was collected and extracted with NaOH solution (pH 14), followed by HCl, and $CHCl_3$. The organic layer was dried over $MgSO_4$ and concentrated as a white solid (80 mg, 60%). ^{1}H NMR (400 MHz, $CDCl_3$) δ 7.24−8.12 (m, 10H, aromatic), 4.89−4.91 (m, 2H, H1 and -CH_2Ph), 4.80−4.83 (m, 2H, -CH_2Ph), 4.66 (d, 1H, J = 10.8 Hz, -CH_2Ph), 4.24 (d, 1H, J = 9.6 Hz, H5), 3.96 (t, 1H, J = 9.6 Hz, H3), 3.75 (t, 1H, J = 9.6 Hz, H4), 3.70 (t, 2H, J = 6.4, Ha), 3.46−3.50 (m, 3H, H2 and −OCH_3), 2.46−2.50 (m, 2H, Hc), 1.95 (quintet, 2H, J = 6.4, Hb); ^{13}C NMR (100 Hz, $CDCl_3$) δ 178.33 (C, -COOH), 173.18 (C, -COOH), 138.31 (C, aromatic), 137.43 (C, aromatic), 130.18 (CH, aromatic), 128.41 (CH, aromatic), 128.12 (CH, aromatic), 127.94 (CH, aromatic), 127.81 (CH, aromatic), 127.74 (CH, aromatic), 98.23 (CH, C1), 81.18 (CH, C3), 80.24 (CH, C2), 79.06 (CH, C4), 75.80 (CH_2, -CH_2Ph), 75.25 (CH_2, -CH_2Ph), 70.16 (CH_2, Ca), 69.54 (CH_1, C5), 55.76 (CH_3, -OCH_3), 30.37 (CH_2, *Cc*), 25.03 (CH_2, Cb); *m/z* 475.1963 (M + H)$^+$, 497.1782 (M + Na)$^+$.

Prodrug 4 (4). The mixture of **18** (15 mg, 0.0115 mmol) and Pd/C (15 mg) in MeOH (2 mL) was stirred at room temperature in hydrogen for 18 h. After filtering by celite and silica gel, the residue was concentrated and recrystallized to give the white solid of prodrug **4** (12 mg, 90%). ^{1}H NMR (400 MHz, $CDCl_3$) δ 7.26−8.14 (m, 15H, aromatic), 7.10 (d, 1H, J = 9.2 Hz, NH), 6.33 (s, 1H, H10), 6.22 (t, 1H, J = 8.9 Hz, H13), 5.97 (dd, 1H, J = 9.2, 2.8 Hz, H3′), 5.69 (d, 1H, J = 7.0 Hz, H2), 5.54 (d, 1H, J = 3.8 Hz, H2′), 4.96−4.98 (m, 1H, H5), 4.83 (d, 1H, J = 3.6 Hz, H1″), 4.41−4.43 (m, 2H, H7 and H5″), 4.31 (d, 1H, J = 8.4 Hz, H20), 4.20 (d, 1H, J = 8.4 Hz, H20), 3.75−3.82 (m, 3H, H3, H3″, and H4″), 3.66−3.71 (m, 1H, Ha), 3.38−3.44 (m, 4H, Ha and −OCH_3), 3.31 (dd, 1H, J = 8.8, 3.6 Hz), 2.67−2.70 (m, 1H, Hc), 2.54−2.60 (m, 1H, H6), 2.45 (s, 3H, 4-$OCOCH_3$), 2.32−2.45 (m, 2H, H14 and Hc), 2.25 (s, 3H, 10-$OCOCH_3$), 2.13−2.17 (m, 1H, H14), 1.93 (s, 3H, H18), 1.90−1.93 (m, 3H, H6 and Hb), 1.69 (s, 3H, H19), 1.24 (s, 3H, H16), 1.14 (s, 3H, H17); ^{13}C NMR (100 Hz, $CDCl_3$) δ 203.70 (C, C9), 176.76 (C, -COOR), 172.61 (C, -COOR), 171.20 (C, -COOR), 169.88 (C, -COOR), 168.51 (C, -COOR), 167.17 (C, -COOR), 167.01 (C, -COOR), 152.71 (C or CH, aromatic or C11 or C12), 142.37 (C or CH, aromatic or C11 or C12), 136.86 (C or CH, aromatic or C11 or C12), 133.65 (C or CH, aromatic or C11 or C12), 133.01 (C or CH, aromatic or C11 or C12), 132.00 (C or CH, aromatic or C11 or C12), 130.20 (C or CH, aromatic or C11 or C12), 129.22 (C or CH, aromatic or C11 or C12), 129.08 (C or CH, aromatic or C11 or C12), 128.70 (C or CH, aromatic or C11 or C12), 128.51 (C or CH, aromatic or C11 or C12), 127.20 (C or CH, aromatic or C11 or C12), 126.60 (C or CH, aromatic or C11 or C12), 98.06 (CH, C1″), 84.42 (CH,C5), 81.13 (C, C4), 79.80 (CH, C2″), 79.13 (C,C1), 75.56 (CH,C10), 75.07 (CH, C2), 74.09 (CH, C2′), 72.75 (CH, C3″ and C4″), 72.07 (CH, C7 and C13), 71.99 (CH, C7 and C13), 68.73 (CH_2, Ca), 68.13 (CH, C5″), 58.41 (C, C8), 55,91 (CH_3, -OCH_3), 52.77 (CH, C3′), 45.69 (CH, C3), 43.17 (C, C15), 35.62 (CH, C6 and C14), 29.84 (CH_2, *Cc*), 26.84 (CH_3, C16), 24.75 (CH_2, Cb), 22.64 (CH_3, 4-$OCOCH_3$), 22.05 (CH_3, C17), 20.84 (CH_3, 10-$OCOCH_3$), 14.89 (CH_3, C18), 9.64 (CH_3, C19).

Synthesis of Fluorescence-Labeled Prodrug. The synthesis of fluorescence-labeled prodrug, C16-F, was performed in five steps (Scheme 5).

Paclitaxel-2′TES (19). The mixture of paclitaxel (100 mg, 0.117 mmol) and chlorotriethylsilane (19.4 mg, 0.1287 mmol) in pyridine was stirred at room temperature for 3 h. After quenching by the addition of water, the mixture was extracted with EtOAc (15 mL × 3), dried over $MgSO_4$, and concentrated. The residue was purified by silica gel chromatography (EtOAc/Hex = 3/2) and dried under vacuum to produce a white solid (190 mg, 84%). ^{1}H NMR (400 MHz, $CDCl_3$) δ 7.26−8.15 (m, 15H, aromatic, 7.12 (d, 1H, J = 8.9 Hz, NH), 6.25−6.30 (m, 2H, H10 and H13), 5.69−5.73 (m, 2H, H2 and H3′), 4.98 (dd, 1H, J = 9.6, 2.0 Hz, H5), 4.70 (d, 1H, J = 3.4 Hz, H2′), 4.43 (m, 1H, H7), 4.33 (d, 1H, J = 8.4 Hz, H20), 4.23 (d, 1H, J = 8.4 Hz, H20), 3.83 (d, 1H, J = 7.1 Hz, H3), 2.53−2.58 (m, 4H, H6 and 4-$OCOCH_3$.), 2.38−2.44 (m, 1H, H14), 2.23 (s, 3H, 10-$OCOCH_3$), 2.14−2.20 (m, 1H, H14), 1.86−1.93 (m, 4H, H6 and H18), 1.69 (s, 3H, H19), 1.25 (s, 3H, H17), 1.14 (s, 3H, H16), 0.82 (t, 9H, J = 7.9 Hz, $SiCH_2CH_3$), 0.41−0.53 (m, 6H, $SiCH_2CH_3$); ^{13}C NMR (100 Hz, $CDCl_3$) δ 203.74 (C, C9), 171.53 (C, RCOOR′), 171.27 (C, RCOOR′), 170.06 (C, RCOOR′), 166.99 (C, RCOOR′), 142.49 (C, C11 or C13 or aromatic), 138.39 (C, C11 or C13 or aromatic), 134.07 (C, C11 or C13 or aromatic), 133.65 (CH, aromatic), 132.94 (C, C11 or C13 or aromatic), 131.76 (CH, aromatic), 130.21 (CH, aromatic), 129.17 (C, C11 or C13 or aromatic), 128.69 (CH, aromatic), 128.00 (C, C11 or C13 or aromatic), 127.02 (CH, aromatic), 126.45 (CH, aromatic), 84.44 (CH,C5), 81.16 (C, C4), 79.13 (C, C1), 75.55 (CH, C10), 75.10 (CH, C2), 74.87 (CH, C2′), 72.11 (CH,C7), 71.45 (CH, C13), 58.53 (C, C8), 55.69 (CH, C3′), 45.50 (CH, C3), 43.24 (C, C15), 35.82 (CH, C14), 35.55 (CH, C6), 26.76 (CH_3, C17), 22.97 (CH_3, 4-$OCOCH_3$), 22.26 (CH_3, C16), 20.81 (CH_3, 10-$OCOCH_3$), 14.82 (CH_3, C18), 9.61 (CH_3, C19), 6.49 ($SiCH_2CH_3$), 4.37 ($SiCH_2CH_3$); *m/z* 968.4247 (M + H)$^+$.

Paclitaxel-2′TES-7F (20). The mixture of **19** (60 mg, 0.062 mmol), *m*-NHCbz benzoic acid (74 mg, 0.27 mmol), DCC (55 mg, 0.267 mmol), and a catalytic amount of DMAP in THF (2 mL) was stirred at room temperature for 18 h. After concentration, the residue was purified by silica gel chromatography (EtOAc/Hex = 1/2) and dried under vacuum to produce a white solid (35 mg, 46%). ^{1}H NMR (400 MHz, $CDCl_3$) δ 7.31−8.16 (m, 23H, aromatic), 7.13 (d, 1H, J = 8.9 Hz, NH), 6.82 (s, 1H), 6.40 (s, 1H, H10), 6.25 (t, 1H, J = 9.0 Hz, H13), 5.71−5.79 (m, 3H, H2, H7, and H3′), 5.22 (s, 2H, -CH_2Ph), 5.02 (m, 1H, H5), 4.72 (d, 1H, J = 1.9 Hz, H2′), 4.38 (d, 1H, J = 8.4 Hz, H20), 4.16 (d, 1H, J = 8.4 Hz, H20), 4.05 (d, 1H, J = 7.0 Hz, H3), 2.73−2.79 (m, 1H, H6), 2.56 (s, 3H, 4-$OCOCH_3$), 2.43−2.49 (m, 1H, H14), 2.17−2.23 (m, 1H, H14), 2.01 (s, 3H, H18), 1.97 (s, 3H, 10-$OCOCH_3$), 1.92 (s, 3H, H19), 1.21 (s, 3H, H17), 1.18 (s, 3H, H16), 0.83 (t, 9H, J = 3.4 Hz, $SiCH_2CH_3$), 0.44−0.54 (m, 6H, $SiCH_2CH_3$); ^{13}C NMR (100 Hz, $CDCl_3$) δ 202.54 (C, C9), 171.59 (C, RCOOR′), 169.85 (C, RCOOR′), 168.41 (C, RCOOR′), 166.99 (C, RCOOR′), 164.81 (C, RCOOR′), 141.06 (CH, aromatic), 138.43 (CH, aromatic), 137.77 (CH, aromatic), 135.96 (CH, aromatic), 134.14 (CH, aromatic), 133.73 (CH, aromatic), 132.93 (CH, aromatic), 131.74 (CH, aromatic), 130.21 (CH, aromatic), 129.10 (CH, aromatic), 128.79 (CH, aromatic), 128.69 (CH, aromatic), 128.62 (CH, aromatic), 128.31 (CH, aromatic), 127.97 (CH, aromatic), 127.03 (CH, aromatic), 126.46 (CH, aromatic), 124.88 (CH, aromatic), 123.13 (CH, aromatic), 83.99 (CH, C5), 80.95 (C,C4), 78.75 (C, C1), 74.77 (CH, C10 and C2′), 74.64 (CH, C2 or C7 or C3′), 72.23 (CH, C2 or C7 or C3′), 71.33 (CH, C13), 67.12 (CH_2, -CH_2Ph), 56.25 (C,

C8), 55.72 (CH, C2 or C7 or C3′), 46.63 (CH, C3), 43.32 (C, C15), 35.70 (CH, C14), 33.33 (CH, C6), 26.34 (CH_3, C17), 22.93 (CH_3, 4-$OCOCH_3$), 21.48 (CH_3, C16), 20.42 (CH_3, 10-$OCOCH_3$), 14.67 (CH_3, C18), 11.10 (CH_3, C19), 6.48 (CH_3, $SiCH_2CH_3$), 4.37 (CH_2, $SiCH_2CH_3$); *m/z* 1221.4986 $(M + H)^+$, 1243.4805 $(M + Na)^+$.

Paclitaxel-2′OH-7F (21). The mixture of **20** (30 mg, 0.025 mmol) and Bu_4NF (30 μL of 1 M solution in THF, 0.03 mmol) in THF (1 mL) was stirred at room temperature for 2 h. After concentration, the residue was dissolved in EtOAc, extracted with NaCl, dried over $MgSO_4$, and concentrated. The residue was purified by silica gel chromatography (EtOAc/Hex = 3/2) and dried under vacuum to produce a white solid (27 mg, 100%). ^{1}H NMR (400 MHz, $CDCl_3$ δ7.33−8.14 (m, 23H, aromatic), 7.10 (d, 1H, *J* = 8.9 Hz, NH), 6.36 (s, 1H, H10), 6.19 (t, 1H, *J* = 8.8 Hz, H13), 5.82 (dd, 1H, *J* = 8.9, 2.4 Hz, H3′), 5.69−5.74 (m, 2H, H2 and H7), 5.21 (s, 2H, -CH_2Ph), 4.98 (d, 1H, *J* = 8.6 Hz, H5), 4.83 (t, 1H, *J* = 2.4 Hz, H2′), 4.35 (d, 1H, *J* = 8.4 Hz, H20), 4.24 (d, 1H, *J* = 8.4 Hz, H20), 4.01 (d, 1H, *J* = 6.9 Hz, H3), 3.71 (br, 1H, OH), 2.72−2.80 (m, 1H, H6), 2.40 (s, 3H, 4-$OCOCH_3$), 2.35−2.37 (m, 1H, H14), 1.97 (s, 3H, 10-$OCOCH_3$), 1.95 (s, 3H, H16), 1.87−1.90 (m, 4H, H14 and H19), 1.20 (s, 3H, H17), 1.19 (s, 3H, H16); ^{13}C NMR (100 Hz, $CDCl_3$) δ 202.42 (C, C9), 172.52 (C, RCOOR′), 170.35 (C, RCOOR′), 168.41 (C, RCOOR′), 167.02 (C, RCOOR′), 166.91 (C, RCOOR′), 164.82 (C, RCOOR′), 153.24 (C, aromatic), 140.46 (C, aromatic), 138.02 (C, aromatic), 137.81 (C, aromatic), 135.97 (C, aromatic), 133.77 (C, aromatic), 133.68 (C, aromatic), 133.22 (C, aromatic), 131.94 (C, aromatic), 130.82 (C, aromatic), 130.18 (C, aromatic), 129.09 (C, aromatic), 128.99 (C, aromatic), 128.71 (C, aromatic), 128.62 (C, aromatic), 128.30 (C, aromatic), 127.04 (C, aromatic), 124.83 (C, aromatic), 123.12 (C, aromatic), 119.74 (C, aromatic), 83.90 (CH, C5), 81.03 (C, C4), 78.57 (C, C1), 74.86 (CH, C10), 74.43 (CH, C2), 73.17 (CH, C2′), 72.26 (CH, C7 or C13), 72.28 (CH, C7 or C13), 67.11 (CH_2, -CH_2Ph), 56.37 (C, C8), 54.90 (CH, C3′), 46.78 (CH, C3), 43.22 (C, C15), 35.65 (CH, C14), 33.38 (CH, C6), 26.49 (CH_3, C17), 22.54 (CH_3, 4-$OCOCH_3$), 20.94 (CH_3, C16), 20.45 (CH_3, 10-$OCOCH_3$), 14.09 (CH_3, C18), 11.03 (CH_3, C19); *m/z* 1107.4121 $(M + H)^+$, 1129.3941 $(M + Na)^+$.

Fluorescence-Labeled Prodrug 1 (22). The mixture of **21** (30 mg, 0.027 mmol), **5** (17 mg, 0.035 mmol), DCC (9 mg, 0.041 mmol), and a catalytic amount of DMAP in THF (1 mL) was stirred at room temperature for 18 h. After concentration, the residue was purified by silica gel chromatography (EtOAc/Hex = 1/1) and dried under vacuum to produce a white solid (36 mg, 85%). ^{1}H NMR (400 MHz, $CDCl_3$) δ 7.24−8.14 (20H, m, aromatic), 7.09 (1H, d, *J* = 9.0 Hz, NH), 6.43 (1H, s, H10), 6.16 (1H, t, *J* = 8.2 Hz, H13), 5.93 (1H, dd, *J* = 9.0, 4.1 Hz, H3′), 5.73 (1H, d, *J* = 6.9 Hz, H2), 5.68 (1H, dd, *J* = 10.4, 7.2 Hz, H7), 5.54 (1H, d, *J* = 4.1 Hz, H2′), 5.00 (1H, d, *J* = 8.3 Hz, H5), 4.82 (1H, d, *J* = 3.6 Hz, H1″), 4.70 (1H, dd, *J* = 9.7 Hz, H2″), 4.34 (1H, d, *J* = 8.4 Hz, H20), 4.22 (1H, d, *J* = 8.4 Hz, H20), 4.00 (1H, d, *J* = 6.9 Hz, H3), 3.94 (1H, t, *J* = 9.7 Hz, H3″), 3.79−3.83 (2H, m, H6″), 3.61−3.65 (1H, m, H5″), 3.52 (1H, t, *J* = 9.7 Hz, H4″), 3.37 (3H, s, -OCH_3), 2.66−2.86 (5H, m, H6 and succinic), 2.43 (3H, s, 4-$OCOCH_3$), 2.28−2.34 (1H, m, H14), 2.08−2.17 (1H, m, H14), 2.01 (3H, s, H18), 1.99 (3H, s, 10-$OCOCH_3$), 1.88−1.91 (4H, m, H6 and H19), 1.18 (6H, s, H16 and H17); ^{13}C NMR (100 Hz, $CDCl_3$) δ 202.36 (C, C9), 171.80 (C, RCOOR′), 171.64 (C, RCOOR′), 169.83 (C, RCOOR′), 168.38 (C, RCOOR′), 168.11 (C, RCOOR′), 167.20 (C, RCOOR′), 166.98 (C, RCOOR′), 166.22 (C, RCOOR′), 150.26 (C), 141.15 (C or CH, aromatic or C11 or C12), 136.81 (C or CH, aromatic or C11 or C12), 133.76 (C or CH, aromatic or C11 or C12), 132.88 (C or CH, aromatic or C11 or C12), 132.00 (C or CH, aromatic or C11 or C12), 130.56 (C or CH, aromatic or C11 or C12), 130.18 (C or CH, aromatic or C11 or C12), 129.09 (C or CH, aromatic or C11 or C12), 128.71 (C or CH, aromatic or C11 or C12), 128.58 (C or CH, aromatic or C11 or C12), 127.18 (C or CH, aromatic or C11 or C12), 126.76 (C or CH, aromatic or C11 or C12), 117.95 (C or CH, aromatic or C11 or C12), 116.87 (C or CH, aromatic or C11 or C12), 113.81 (C or CH, aromatic or C11 or C12), 96.99 (CH,C1″), 83.96 (CH, C5), 80.95 (C, C4), 78.76 (C, C1), 76.34 (CH_2, C20), 74.78 (CH, C10), 74.62 (CH, C2), 74.39 (CH, C2′), 73.79 (CH, C2″), 72.22 (CH, C7), 71.88 (CH, C13), 71.67 (CH, C3″), 71.19 (CH, C4″), 70.84 (CH, C5″), 62.29 (CH, C6″), 56.28 (C, C8), 55.18 (CH_3, -OCH_3), 53.14 (CH, C3′), 46.73 (CH, C3), 43.19 (C, C15), 35.31 (CH_2, C14), 33.23 (CH_2, C6), 29.16 (CH_2, Cb or *Cc*), 29.07 (CH_2, Cb or *Cc*), 26.38 (CH_3, C17), 22.59 (CH_3, 4-$OCOCH_3$), 21.26 (CH_3, C16), 20.45 (CH_3, 10-$OCOCH_3$), 14.53 (CH_3, C18), 11.03 (CH_3, C19).

C16-F (23). The mixture of **22** (46 mg, 0.029 mmol) and Pd/C (25 mg) in MeOH (4 mL) was stirred at room temperature in hydrogen for 12 h. The solution was filtered by celite and silica gel. The residue was concentrated and recrystallized to give a white solid of fluorescence-labeled prodrug **23** (35 mg, 96.6%). ^{1}H NMR (400 MHz, $CDCl_3$) δ 7.24−8.14 (20H, m, aromatic), 7.09 (1H, d, *J* = 9.0 Hz, NH), 6.43 (1H, s, H10), 6.16 (1H, t, *J* = 8.2 Hz, H13), 5.93 (1H, dd, *J* = 9.0, 4.1 Hz, H3′), 5.73 (1H, d, *J* = 6.9 Hz, H2), 5.68 (1H, dd, *J* = 10.4, 7.2 Hz, H7), 5.54 (1H, d, *J* = 4.1 Hz, H2′), 5.00 (1H, d, *J* = 8.3 Hz, H5), 4.82 (1H, d, *J* = 3.6 Hz, H1″), 4.70 (1H, dd, *J* = 9.7 Hz, H2″), 4.34 (1H, d, *J* = 8.4 Hz, H20), 4.22 (1H, d, *J* = 8.4 Hz, H20), 4.00 (1H, d, *J* = 6.9 Hz, H3), 3.94 (1H, t, *J* = 9.7 Hz, H3″), 3.79−3.83 (2H, m, H6″), 3.61v3.65 (1H, m, H5″), 3.52 (1H, t, *J* = 9.7 Hz, H4″), 3.37 (3H, s, -OCH_3), 2.66−2.86 (5H, m, H6 and succinic), 2.43 (3H, s, 4-$OCOCH_3$), 2.28−2.34 (1H, m, H14), 2.08−2.17 (1H, m, H14), 2.01 (3H, s, H18), 1.99 (3H, s, 10-$OCOCH_3$), 1.88−1.91 (4H, m, H6 and H19), 1.18 (6H, s, H16 and H17); ^{13}C NMR (100 Hz, $CDCl_3$) δ 202.36 (C, C9), 171.80 (C, RCOOR′), 171.64 (C, RCOOR′), 169.83 (C, RCOOR′), 168.38 (C, RCOOR′), 168.11 (C, RCOOR′), 167.20 (C, RCOOR′), 166.98 (C, RCOOR′), 166.22 (C, RCOOR′), 150.26 (C), 141.15 (C or CH, aromatic or C11 or C12), 136.81 (C or CH, aromatic or C11 or C12), 133.76 (C or CH, aromatic or C11 or C12), 132.88 (C or CH, aromatic or C11 or C12), 132.00 (C or CH, aromatic or C11 or C12), 130.56 (C or CH, aromatic or C11 or C12), 130.18 (C or CH, aromatic or C11 or C12), 129.09 (C or CH, aromatic or C11 or C12), 128.71 (C or CH, aromatic or C11 or C12), 128.58 (C or CH, aromatic or C11 or C12), 127.18 (C or CH, aromatic or C11 or C12), 126.76 (C or CH, aromatic or C11 or C12), 117.95 (C or CH, aromatic or C11 or C12), 116.87 (C or CH, aromatic or C11 or C12), 113.81 (C or CH, aromatic or C11 or C12), 96.99 (CH,C1″), 83.96 (CH, C5), 80.95 (C, C4), 78.76 (C, C1), 76.34 (CH_2, C20), 74.78 (CH, C10), 74.62 (CH, C2), 74.39 (CH, C2′), 73.79 (CH, C2″), 72.22 (CH, C7), 71.88 (CH, C13), 71.67 (CH, C3″), 71.19 (CH, C4″), 70.84 (CH, C5″), 62.29 (CH, C6″), 56.28 (C, C8), 55.18 (CH_3, -OCH_3), 53.14 (CH, C3′), 46.73 (CH, C3), 43.19 (C, C15), 35.31 (CH_2, C14), 33.23 (CH_2, C6), 29.16 (CH_2, Cb or *Cc*), 29.07 (CH_2, Cb or *Cc*), 26.38 (CH_3, C17), 22.59 (CH_3, 4-$OCOCH_3$), 21.26 (CH_3, C16), 20.45 (CH_3, 10-$OCOCH_3$), 14.53 (CH_3, C18), 11.03 (CH_3, C19).

Biology. Cell Cultures. NCI-H838 nonsmall lung cancer cells (lung adenocarcinoma) were maintained in DMEM medium with 10% FBS, 2 mM glutamine, and antibiotics (100 units/mL penicillin and 100 μg/mL streptomycin). Hep-3B hepatoma cells were maintained in MEME containing 10% FBS. A498 renal cancer cells were maintained in 90% MEME medium supplemented with 1 mM sodium pyruvate, 10% FCS, and antibiotics. MES-SA uterine cancer cells were maintained in McCoy's 5A medium supplemented with 10% FCS, 25 mM HEPES, 2 mM L-glutamine, and antibiotics. HCT-116 colon cancer cells were maintained in McCoy's 5A medium supplemented with 10% heat-inactivated FBS. NPC-TW01 nasopharynx cancer cells were maintained in DMEM medium supplemented with 10% FBS and antibiotics. MKN-45 gastric cancer cells were maintained in RPMI-1640 medium supplemented with 10% FBS and antibiotics. HUV-EC-C human umbilical vein endothelial cells were maintained in Ham's F12K medium supplemented with 50 μg/mL endothelial growth factors, 12% FBS, and antibiotics. CHO-K1 Chinese hamster ovary cells were maintained in Ham's F12K medium with 10% FBS and antibiotics. All cell lines were cultured in an incubator with humidified 5% CO_2/95% air at 37 °C.

Cell Proliferation Assay. Cell proliferation assays were conducted to measure and compare the cytotoxicity and selectivity of

these prodrugs and their parent drug paclitaxel. Cells (2×10^4 cells/well) were seeded onto a 96-well plate before 12 h of drug treatment. Stock drug solutions were serially diluted and administrated to cells at final concentrations of 0.5 nM to 10 μM. After 72 h, the medium was removed and replaced with fresh media. Ten microliters of MTT (5 mg/mL) solution was added to each well. After 4 h incubation at 37 °C, the MTT solution was aspirated and 100 μL of DMSO was added to dissolve the dye precipitated in cells. The absorbance of each sample was recorded at a wavelength of 570 nm on a DYNEX MRX II. The percentage of viable cells at different concentrations of prodrugs was plotted relative to control values, and the IC_{50} values were computed. The IC_{50} value was defined as the concentration required to inhibit cell growth by 50% relative to untreated cancer growth. This value was determined after 72-h treatment.

RNA Extraction and RT-PCR of GLUTs. Total RNA from 9 cell lines was isolated by High Pure RNA Isolation Kit, according to the manufacturer's instruction. The sequence primers used were (1) GLUT1, forward 5′-CGGGCCAAGAGTGTGCTAAA-3′ (846−865), reverse 5′-TGACGATACCGGAGCCAATG-3′ (1109−1128), 283 bp PCR product; (2) GLUT4, forward 5′-CCCCCTCAGCAGCGAGTGA-3′ (188−206), reverse 5′-GCACCGCCAGGACATTGTTG-3′ (487−506), 319 bp PCR product; (3) β-actin, forward 5′-GTGGGGCGCCCCAGGCACCA-3′ (176−196), reverse 5′-TCCTTAATGTCACGCACGATTTC-3′ (692−714), 539 bp PCR product. PCR was carried out with a Px2 Thermal Cycler. The PCR condition was to heat at 94 °C for 1 min, followed by denaturation at 94 °C for 1 min, annealing at 60 °C for 1 min, extension at 72 °C for 1 min for 35 cycles, and finally incubation at 72 °C for 10 min. The PCR products were separated on 1.5% agarose gel and visualized with ethidium bromide.

Inhibition of GLUTs by Phloretin. NPC-TW01 cells were cultured on coverslips. After 12 h, cells were pretreated with phloretin (100 μM) for 10 min and subsequently treated with prodrug **1** (100 μM) for 30 min. After washing twice with PBS, cells were fixed with 4% paraformaldehyde for 30 min, mounted with ProLong Gold antifade reagent, and analyzed with fluorescence microscope.

Fluorescence Microscopy. NPC-TW01 cells were cultured on coverslips coated with poly-D-Lys (0.1 mg/mL) for 12 h and then treated with fluorescence-labeled prodrug **1** (100 μg/mL), paclitaxel (100 μg/mL), or DMSO (0.1%) for 5 h. Cells were washed twice with PBS and fixed with 4% formaldehyde for 30 min. After washing with PBS, fixed cells were mounted with ProLong Gold antifade reagent and analyzed with fluorescence microscope.[42]

Confocal Microscopy. NPC-TW01 cells cultured on coverslips were treated with paclitaxel and prodrugs (1 μM) for 24 h. After washing twice with PBS, cells were fixed with 4% paraformaldehyde, permeabilized with 0.1% Triton-X100, and blocked with 0.1% BSA. For tubulin morphology examination, cells were incubated with the monoclonal anti-β-tubulin antibody (diluted to 1:200 with PBS) for 45 min at room temperature. After five washings with PBS, the anti-tubulin antibody treated cells were incubated with PE-labeled goat anti-mouse IgG antibody (diluted to 1:100 with PBS) for 45 min at room temperature.[43] After that, coverslips were washed with PBS, mounted onto microscopic slides, and analyzed with the Carl Zeiss Laser Scanning System LSM 510. To observe chromosome morphology, cells treated with drugs were fixed with 4% paraformaldehyde, and stained with Hoechst 33258.[44] After five washings with PBS, cells were mounted onto slides, and analyzed with confocal microscopy.

Quantification of Prodrug Uptake by RP-HPLC. NPC-TW01 cells (2×10^4 cells) were seeded onto 10 cm-culture dish before 12 h of drug treatment. The cell cultured medium was changed to either medium with or without FBS (serum-free medium). The cells were treated with 100 μM prodrug **1** and incubated at 37 °C for 4, 8, and 24 h. The cell cultured medium was collected and extracted with 10 mL of dichloromethane four times. The extracts were rehydrated with sodium sulfate anhydrous and evaporated by vacuum evaporator. The dry extracts were resuspended in 400 μL of methanol and the prodrug **1** uptake was determined by RP-HPLC. Analysis of prodrug **1** or paclitaxel in medium was performed using a RP-HPLC column (4.6 × 150 mm, Supelco Ascentis C18 column, 5 μm particle size). The mobile phase was prepared as follows: mobile phase A, 95% distilled water and 5% ACN; mobile phase B, 100% ACN, then filtered through a 0.22-μm Millipore filter and degassed before use. The sample was eluted with an isocratic elution of 60% A and 40% B. The HPLC condition was used for 20 min running time at a flow rate of 1 mL/min. The eluent was monitored at 220 nm. For the quantification of prodrug uptake in NPC-TW01 cells in the presence and absence of 100 μM phloretin, the cells were pretreated with 100 μM phloretin for 1 h and followed with 100 μM prodrug **1**. After 24 h, the prodrug **1** was extracted and analyzed on RP-HPLC as described above. The standard mixture of prodrug **1** and paclitaxel with different equal concentrations at 1.25, 2.5, 5 and 10 μM were used to calculate the prodrug **1** or paclitaxel content in cell cultured medium or serum-free medium.

Acknowledgment. We gratefully thank Dr. C. C. Hung for his helpful instruction with the confocal microscopy and Dr. S. C. Jao for his helpful instruction with the nuclear magnetic resonance (NMR) spectroscopy. This work is supported by the Graduate School, Chiang Mai University, Chiang Mai, Thailand.

Supporting Information Available: Analysis of prodrugs **1**−**4** by RP-HPLC and MS; RT-PCR result of GLUT expression level in 9 cell lines; cytotoxic activity of prodrug **1** with/without phloretin against NPC-TW01 cells. This material is available free of charge via the Internet at http://pubs.acs.org.

References

(1) Shen, S. I.; Kotamraj, P. R.; Bhattacharya, S.; Li, X.; Jasti, B. R. Synthesis and characterization of RGD-fatty acid amphiphilic micelles as targeted delivery carriers for anticancer agents. *J. Drug Target* **2007**, *15*, 51–58.

(2) Mittal, S.; Song, X.; Vig, B. S.; Amidon, G. L. Proline prodrug of melphalan targeted to prolidase, a prodrug activating enzyme overexpressed in melanoma. *Pharm. Res.* **2007**, *24*, 1290–1298.

(3) Sperker, B.; Werner, U.; Murdter, T. E.; Tekkaya, C.; Fritz, P.; Wacke, R.; Adam, U.; Gerken, M.; Drewelow, B.; Kroemer, H. K. Expression and function of beta-glucuronidase in pancreatic cancer: potential role in drug targeting. *Naunyn-Schmiedeberg's Arch. Pharmacol.* **2000**, *362*, 110–115.

(4) Bosslet, K.; Straub, R.; Blumrich, M.; Czech, J.; Gerken, M.; Sperker, B.; Kroemer, H. K.; Gesson, J. P.; Koch, M.; Monneret, C. Elucidation of the mechanism enabling tumor selective prodrug monotherapy. *Cancer Res.* **1998**, *58*, 1195–1201.

(5) Islam, M. R.; Tomatsu, S.; Shah, G. N.; Grubb, J. H.; Jain, S.; Sly, W. S. Active site residues of human beta-glucuronidase. Evidence for Glu(540) as the nucleophile and Glu(451) as the acid-base residue. *J. Biol. Chem.* **1999**, *274*, 23451–23455.

(6) Liu, D. Z.; Sinchaikul, S.; Reddy, P. V.; Chang, M. Y.; Chen, S. T. Synthesis of 2′-paclitaxel methyl 2-glucopyranosyl succinate for specific targeted delivery to cancer cells. *Bioorg. Med. Chem. Lett.* **2007**, *17*, 617–620.

(7) Funasaka, T.; Yanagawa, T.; Hogan, V.; Raz, A. Regulation of phosphoglucose isomerase/autocrine motility factor expression by hypoxia. *FASEB J.* **2005**, *19*, 1422–1430.

(8) Macheda, M. L.; Rogers, S.; Best, J. D. Molecular and cellular regulation of glucose transporter (GLUT) proteins in cancer. *J. Cell. Physiol.* **2005**, *202*, 654–662.

(9) Ettmayer, P.; Amidon, G. L.; Clement, B.; Testa, B. Lessons learned from marketed and investigational prodrugs. *J. Med. Chem.* **2004**, *47*, 2393–2404.

(10) Skwarczynski, M.; Hayashi, Y.; Kiso, Y. Paclitaxel prodrugs: toward smarter delivery of anticancer agents. *J. Med. Chem.* **2006**, *49*, 7253–7269.

(11) Damen, E. W.; Nevalainen, T. J.; van den Bergh, T. J.; de Groot, F. M.; Scheeren, H. W. Synthesis of novel paclitaxel prodrugs designed for bioreductive activation in hypoxic tumour tissue. *Bioorg. Med. Chem.* **2002**, *10*, 71–77.

(12) Abouzied, M. M.; Crawford, E. S.; Nabi, H. A. 18F-FDG imaging: pitfalls and artifacts. *J. Nucl. Med. Technol.* **2005**, *33*, 145–155.

(13) Nguyen, X. C.; Lee, W. W.; Chung, J. H.; Park, S. Y.; Sung, S. W.; Kim, Y. K.; So, Y.; Lee, D. S.; Chung, J. K.; Lee, M. C.; Kim, S. E. FDG uptake, glucose transporter type 1, and Ki-67 expressions in non-small-cell lung cancer: correlations and prognostic values. *Eur. J. Radiol.* **2007**, *62*, 214–219.

(14) Ferlini, C.; Ojima, I.; Distefano, M.; Gallo, D.; Riva, A.; Morazzoni, P.; Bombardelli, E.; Mancuso, S.; Scambia, G. Second generation taxanes: from the natural framework to the challenge of drug resistance. *Curr. Med. Chem. Anticancer Agents* **2003**, *3*, 133–138.

(15) Nabholtz, J. M.; Vannetzel, J. M.; Llory, J. F.; Bouffette, P. Advances in the use of taxanes in the adjuvant therapy of breast cancer. *Clin. Breast Cancer* **2003**, *4*, 187–192.

(16) Kumar, N. Taxol-induced polymerization of purified tubulin. Mechanism of action. *J. Biol. Chem.* **1981**, *256*, 10435–10441.

(17) Parekh, H.; Simpkins, H. The transport and binding of taxol. *Gen. Pharmacol.* **1997**, *29*, 167–172.

(18) Horwitz, S. B. Mechanism of action of taxol. *Trends Pharmacol. Sci.* **1992**, *13*, 134–136.

(19) Rooseboom, M.; Commandeur, J. N.; Vermeulen, N. P. Enzyme-catalyzed activation of anticancer prodrugs. *Pharmacol. Rev.* **2004**, *56*, 53–102.

(20) Abraham, S.; Guo, F.; Li, L. S.; Rader, C.; Liu, C.; Barbas, C. F.; Lerner, R. A.; Sinha, S. C. Synthesis of the next-generation therapeutic antibodies that combine cell targeting and antibody-catalyzed prodrug activation. *Proc. Natl. Acad. Sci. U.S.A.* **2007**, *104*, 5584–5589.

(21) Chatterjee, S. K.; Zetter, B. R. Cancer biomarkers: knowing the present and predicting the future. *Future Oncol.* **2005**, *1*, 37–50.

(22) de Graaf, M.; Boven, E.; Scheeren, H. W.; Haisma, H. J.; Pinedo, H. M. Beta-glucuronidase-mediated drug release. *Curr. Pharm. Des.* **2002**, *8*, 1391–1403.

(23) Wu, J.; Liu, Q.; Lee, R. J. A folate receptor-targeted liposomal formulation for paclitaxel. *Int. J. Pharm.* **2006**, *316*, 148–153.

(24) Prestwich, G. D.; Marecak, D. M.; Marecek, J. F.; Vercruysse, K. P.; Ziebell, M. R. Controlled chemical modification of hyaluronic acid: synthesis, applications, and biodegradation of hydrazide derivatives. *J. Controlled Release* **1998**, *53*, 93–103.

(25) Jaracz, S.; Chen, J.; Kuznetsova, L. V.; Ojima, I. Recent advances in tumor-targeting anticancer drug conjugates. *Bioorg. Med. Chem.* **2005**, *13*, 5043–5054.

(26) Younes, M.; Brown, R. W.; Stephenson, M.; Gondo, M.; Cagle, P. T. Overexpression of Glut1 and Glut3 in stage I nonsmall cell lung carcinoma is associated with poor survival. *Cancer* **1997**, *80*, 1046–1051.

(27) Gleadle, J. M.; Ratcliffe, P. J. Induction of hypoxia-inducible factor-1, erythropoietin, vascular endothelial growth factor, and glucose transporter-1 by hypoxia: evidence against a regulatory role for Src kinase. *Blood* **1997**, *89*, 503–509.

(28) Raval, R. R.; Lau, K. W.; Tran, M. G.; Sowter, H. M.; Mandriota, S. J.; Li, J. L.; Pugh, C. W.; Maxwell, P. H.; Harris, A. L.; Ratcliffe, P. J. Contrasting properties of hypoxia-inducible factor 1 (HIF-1) and HIF-2 in von Hippel-Lindau-associated renal cell carcinoma. *Mol. Cell. Biol.* **2005**, *25*, 5675–5686.

(29) Pandit-Taskar, N. Oncologic imaging in gynecologic malignancies. *J. Nucl. Med.* **2005**, *46*, 1842–1850.

(30) Funasaka, T.; Yanagawa, T.; Hogan, V.; Raz, A. Regulation of phosphoglucose isomerase/autocrine motility factor expression by hypoxia. *FASEB J.* **2005**, *19*, 1422–1430.

(31) Isa, A. Y.; Ward, T. H.; West, C. M.; Slevin, N. J.; Homer, J. J. Hypoxia in head and neck cancer. *Br. J. Radiol.* **2006**, *79*, 791–798.

(32) Noguchi, Y.; Sato, S.; Marat, D.; Doi, C.; Yoshikawa, T.; Saito, A.; Ito, T.; Tsuburaya, A.; Yanuma, S. Glucose uptake in the human gastric cancer cell line, MKN28, is increased by insulin stimulation. *Cancer Lett.* **1999**, *140*, 69–74.

(33) Paik, J. Y.; Lee, K. H.; Ko, B. H.; Choe, Y. S.; Choi, Y.; Kim, B. T. Nitric oxide stimulates 18F-FDG uptake in human endothelial cells through increased hexokinase activity and GLUT1 expression. *J. Nucl. Med.* **2005**, *46*, 365–370.

(34) Sako, T.; Naraba, H.; Teraoka, H.; Kitagawa, T. The intrinsic structure of glucose transporter isoforms Glut1 and Glut3 regulates their differential distribution to detergent-resistant membrane domains in non-polarized mammalian cells. *FEBS J.* **2007**, *274*, 2843–2853.

(35) Liu, X. J.; Yang, C.; Gupta, N.; Zuo, J.; Chang, Y. S.; Fang, F. D. Protein kinase C-zeta of GLUT4 translocation through actin remodeling in CHO cells. *J. Mol. Med.* **2007**, *85*, 851–861.

(36) Nelson, J. A.; Falk, R. E. Phloridzin and phloretin inhibition of 2-deoxy-D-glucose uptake by tumor cells in vitro and in vivo. *Anticancer Res.* **1993**, *13*, 2293–2299.

(37) Ferreira, I. A.; Mocking, A. I.; Urbanus, R. T.; Varlack, S.; Wnuk, M.; Akkerman, J. W. Glucose uptake via glucose transporter 3 by human platelets is regulated by protein kinase B. *J. Biol. Chem.* **2005**, *280*, 32625–32633.

(38) Ericsson, A.; Hamark, B.; Powell, T. L.; Jansson, T. Glucose transporter isofrom 4 is expressed in the syncytiotrophoblast of first trimester human placenta. *Hum. Reprod.* **2005**, *20*, 521–530.

(39) Flier, J. S.; Mueckler, M. M.; Usher, P.; Lodish, H. F. Elevated levels of glucose transport and transporter messenger RNA are induced by ras or src oncogenes. *Science* **1987**, *235*, 1492–1495.

(40) Kant, J.; Huang, S.; Wong, H.; Fairchild, C.; Vyas, D.; Farina, V. Studies toward structure-activity relationships of taxol®: synthesis and cytotoxicity of taxol® analogues with C-2′ modified phenylisoserine side chains. *Bioorg. Med. Chem. Lett.* **1993**, *3*, 2471–2474.

(41) de Groot, F. M.; van Berkom, L. W.; Scheeren, H. W. Synthesis and biological evaluation of 2′-carbamate-linked and 2′-carbonate-linked prodrugs of paclitaxel: selective activation by the tumor-associated protease plasmin. *J. Med. Chem.* **2000**, *43*, 3093–3102.

(42) Huang, C. M.; Wu, Y. T.; Chen, S. T. Targeting delivery of paclitaxel into tumor cells via somatostatin receptor endocytosis. *Chem. Biol.* **2000**, *7*, 453–461.

(43) Kovacs, P.; Csaba, G.; Pallinger, E.; Czaker, R. Effects of taxol treatment on the microtubular system and mitochondria of Tetrahymena. *Cell Biol. Int.* **2007**, *31*, 724–732.

(44) Hartfield, P. J.; Mayne, G. C.; Murray, A. W. Ceramide induces apoptosis in PC12 cells. *FEBS Lett.* **1997**, *401*, 148–152.

JM8006257